DOKUZ EYLÜL UNIVERSITY

GRADUATE SCHOOL OF NATURAL AND APPLIED SCIENCES

NANO BIOCHAR PRODUCTION AND ITS EFFECTS ON MECHANICAL PROPERTIES OF MORTAR

by

Mehmet ŞİŞMAN

July, 2023

İZMİR

NANO BIOCHAR PRODUCTION AND ITS EFFECTS ON MECHANICAL PROPERTIES OF MORTAR

A Thesis Submitted to the
Graduate School of Natural and Applied Sciences of Dokuz Eylül University
In Partial Fulfilment of the Requirements for the Degree of Doctor of Philosophy in Nanoscience and Nanoengineering Program

by
Mehmet ŞİŞMAN

July, 2023
İZMİR

Ph.D. THESIS EXAMINATION RESULT FORM

We have read the thesis entitled "**NANO BIOCHAR PRODUCTION AND ITS EFFECTS ON MECHANICAL PROPERTIES OF MORTAR"** completed by **MEHMET ŞİŞMAN** under supervision of **Assoc. Prof. Dr. EGEMEN TEOMETE** and we certify that in our opinion it is fully adequate, in scope and in quality, as a thesis for the degree of Doctor of Philosophy.

……..

Assoc. Prof. Dr. Egemen TEOMETE

Supervisor

……	…….....
Prof. Dr. Jale YANIK	Prof. Dr. Uğur MALAYOĞLU
Thesis Committee Member	Thesis Committee Member
……	…….....
Prof. Dr. Mustafa CAN	Assoc. Prof. Dr. Gözde DUMAN TAÇ
Examining Committee Member	Examining Committee Member

Prof. Dr. Okan FISTIKOĞLU

Director

Graduate School of Natural and Applied Science

ACKNOWLEDGEMENT

I would like to express my sincere gratitude to my advisor, Assoc. Prof. Dr. Egemen TEOMETE, who supported me throughout my Ph.D. program, which I began fifteen years after receiving my master's degree, shared his experiences with me, and gave me support when I needed it.

I would like to sincerely thank Prof. Dr. Jale YANIK and Prof. Dr. Uğur MALAYOĞLU for their guiding contributions during the thesis monitoring meetings.

I would also like to thank Ayşen MISIRLIOĞLU, Abdulvahid ÇELEBİ, and Dr. Sibel OĞUZLAR who always helped me in biochar production and laboratory studies.

I would also like to thank to Izmir Water and Sewerage Administration General Directorate, Batı Anadolu Cement Industry Co. Ltd. (BATIÇİM and BATIBETON), Sika Construction Chemicals Co., and Cigli Ataturk Organized Industrial Zone (AOSB) for providing the materials.

Most importantly, I would like to thank and express my gratitude to my wife Mürüse ERTEN ŞİŞMAN, and my children Görkem and Melisa, who accompanied me on my life path and sacrificed the time I needed to spend with them for my education.

Mehmet ŞİŞMAN

NANO BIOCHAR PRODUCTION AND ITS EFFECTS ON MECHANICAL PROPERTIES OF MORTAR

ABSTRACT

Recently, using biochar as supplementary material in construction applications has increased due to its ability to enhance the mortar's the mechanical characteristics.

The objective of the research was to explore how the addition of nano biochar produced from sewage sludge (both industrial and municipal) and lignocellulosic biomass (apricot kernel shells) affects the workability and mechanical properties of mortar. Biochar, obtained by slow pyrolysis at 500 °C, was ground to sizes smaller than 500 nm and added to the mortar mixture in different volume percentages. The mixtures were cured for 28 days at 20 °C and mechanical tests were carried out.

According to results, the inclusion of 0.06 percent municipal sewage sludge nano biochar and 0.12 percent apricot kernel nano biochar resulted in 23 and 27 percent increase in flexural strength and 100 and 44 percent increase in fracture energies, respectively, compared to the reference mortar. Furthermore, the addition of 0.12 percent sewage sludge nano biochar and 0.04 percent apricot kernel nano biochar increased compressive strength by 17 and 19 percent, and compressive fracture energies by 28 and 45 percent, respectively. With mixed biochar addition, the increase in mechanical properties was less than with biochar alone.

Consequently, the experimental results indicated that municipal sewage sludge and apricot kernel shell nano biochars have the potential to improve the mechanical properties of the mortar. In addition, using biochar in cementitious composites also enables recycling waste while contributing to mitigating global warming by sequestering carbon.

Keywords: Nano biochar, sewage sludge, apricot kernel shell, pyrolysis, mortar, mechanical properties.

NANO BİYOKÖMÜR ÜRETİMİ VE HARCIN MEKANİK ÖZELLİKLERİNE ETKİLERİ

ÖZ

Son zamanlarda, inşaat uygulamalarında tamamlayıcı malzeme olarak biyokömür kullanımı, harcın mekanik özelliklerini geliştirme kabiliyeti nedeniyle artmıştır.

Araştırmanın amacı, arıtma çamurundan (hem endüstriyel hem de kentsel) ve lignoselülozik biyokütleden (kayısı çekirdeği kabukları) üretilen nano biyokömür ilavesinin harcın işlenebilirliğini ve mekanik özelliklerini nasıl etkilediğini araştırmaktır. 500°C'de yavaş piroliz ile elde edilen biyokömür, 500 nm'den daha küçük boyutlara öğütülmüş ve farklı hacim yüzdelerinde harç karışımına eklenmiştir. Karışımlar, 20 °C'de 28 gün boyunca kürlenmiş ve mekanik testler gerçekleştirilmiştir.

Sonuçlara göre, yüzde 0,06 kanalizasyon çamuru nano biyokömürü ve yüzde 0,12 kayısı çekirdeği nano biyokömürü ilavesi, referans harca kıyasla eğilme mukavemetinde sırasıyla yüzde 23 ve 27'lik bir artış ve kırılma enerjilerinde yüzde 100 ve 44'lük bir artışa neden olmuştur. Ayrıca, yüzde 0,12 oranında arıtma çamuru nano biyokömürü ve yüzde 0,04 oranında kayısı çekirdeği nano biyokömürü ilavesi basınç dayanımını sırasıyla yüzde 17 ve 19, basınç kırılma enerjilerini ise yüzde 28 ve 45 oranında artırmıştır. Karışık biyokömür ilavesi ile mekanik özelliklerdeki artış tek başına biyokömüre göre daha az olmuştur.

Sonuç olarak, deneysel sonuçlar kanalizasyon arıtma çamuru ve kayısı çekirdeği kabuğu nano biyokömürlerinin harcın mekanik özelliklerini artırma potansiyeline sahip olduğunu göstermiştir. Ayrıca, çimentolu kompozitlerde biyokömür kullanımı atıkların geri dönüştürülmesini sağlarken karbonu tutarak küresel ısınmanın azaltılmasına da katkıda bulunmaktadır.

Anahtar Kelimeler: Nano biyokömür, kanalizasyon çamuru, kayısı çekirdeği kabuğu, piroliz, harç, mekanik özellikler.

CONTENTS

Page

Ph.D. THESIS EXAMINATION RESULT FORM ii

ACKNOWLEDGEMENT iii

ABSTRACT iv

ÖZ v

LIST OF FIGURES viii

LIST OF TABLES xi

LIST OF SYMBOLS xii

ABBREVIATIONS xiv

CHAPTER ONE - INTRODUCTION 1

1.1 Background 1
1.2 Objective 4
1.3 Organization of the Research 4

CHAPTER TWO – LITERATURE REVIEW 6

2.1 Properties of Biochar 6
2.2 Production Methods of Biochar 8
2.2.1 Pyrolysis 8
2.2.1.1 Slow Pyrolysis 9
2.2.1.2 Fast Pyrolysis 9
2.2.1.3 Flash Pyrolysis 9
2.2.2 Torrefaction 11
2.2.3 Hydrothermal Carbonization 11
2.2.4 Gasification 12
2.2.5 Flash Carbonization 12
2.3 Biochar Usage Areas 16

2.4 Nano Biochar Production 19
2.5 Effect of Biochar on Mortar or Concrete's Mechanical Properties 20

CHAPTER THREE – MATERIALS AND METHODS 25

3.1 Materials 25
3.1.1 Cement and Sand 25
3.1.2 Water 26
3.1.3 Superplasticizer 26
3.1.4 Biochar Production 26
3.2 Methods 31
3.2.1 Characterization of Raw Material and Nano Biochar 31
3.2.2 Mortar Mixture's Preparation 33
3.2.2.1 Mortar Mixture's Design 33
3.2.2.2 Mortar Mixing, Flow Test 33
3.2.3 Molding, Curing 37
3.2.4 Testing of the Mortar Samples 38
3.2.4.1 Flexural Test 40
3.2.4.2 Compression Test 41

CHAPTER FOUR – RESULTS AND DISCUSSION 43

4.1 Biochar Properties 43
4.2 Flow of Mortar Mixtures 45
4.3 Flexural Strength and Energy of Mortar Blocks 47
4.4 Compressive Strength and Energy of Mortar Blocks 53
4.5 Micro Structural Analysis by SEM-EDS of Mortar 60

CHAPTER FIVE- CONCLUSIONS AND FUTURE PLANS 66

5.1 Conclusions 66
5.2 Future Plan 68

REFERENCES 69

LIST OF FIGURES

Page

Figure 2.1 Schematic representation of biochar structure (Ok, Uchimiya, Chang, & Bolan, 2015) 7
Figure 2.2 Biochar structure development during pyrolysis (Lehmann & Joseph, 2009) 10
Figure 2.3 Biochar production methods with common feedstock types (Vithanage et al., 2017) 15
Figure 2.4 Biochar application areas (Carvalho et al., 2022) 16
Figure 2.5 Benefits of biochar in farming and forestry systems (Wang et al., 2020) 17
Figure 2.6 The impacts of biochar produced by pyrolysis on global climate (Woolf, Amonette, Street-Perrott, Lehmann, & Joseph, 2010) 18
Figure 2.7 The nano biochar preparation process (Ramanayaka et al., 2020) 20
Figure 3.1 The raw material of (a-b-c) industrial chemical sludge (d) industrial mixed sludge (e) dried municipal sewage sludge (f) dried apricot kernel shell (Personal archive, 2019) 27
Figure 3.2 Pyrolysis experiment: (a) vertical reactor (b) nitrogen gas (c) thermocouple (d) liquid collection flasks (e) gas products (Personal archive, 2019) 28
Figure 3.3 Raw material and produced biochar (a) industrial chemical sludge (b) industrial chemical sludge biochar (c) industrial mixed sludge (d) industrial mixed sludge biochar (e) municipal sewage sludge (f) municipal sewage sludge biochar (g) apricot kernel shell (h) apricot kernel shell biochar (Personal archive, 2019) 30
Figure 3.4 Determination of density process 32
Figure 3.5 Dispersion process (Personal archive, 2020) 35
Figure 3.6 Mortar mixing with 5-liter capacity mixer (Personal archive, 2020) 36
Figure 3.7 Mortar flow test (Personal archive, 2020) 37
Figure 3.8 Molding (a) molds (b) specimens after 24 hours from the molds (Personal archive, 2020) 38
Figure 3.9 Curing tank (Personal archive, 2020) 38
Figure 3.10 Shimadzu testing machine (Personal archive, 2020) 39

Figure 3.11 Three-point flexural test of mortar samples (Personal archive, 2020) ... 40
Figure 3.12 Compression test of mortar samples (Personal archive, 2020)..... 42
Figure 4.1 SEM images of (a) industrial chemical sludge nano biochar (b) industrial mixed sludge nano biochar (c) sewage sludge nano biochar (d) apricot kernel shell nano biochar..... 44
Figure 4.2 Flow of mortar mixtures with (a) different volume of nano biochar (b) different combinations of apricot kernel shell nano biochar and sewage sludge nano biochar (c) different raw material by 0.12 volume %..... 46
Figure 4.3 Flexural strength of mortar mixtures with (a) different volume of nano biochar (b) different combinations of apricot kernel shell nano biochar and sewage sludge nano biochar (c) different raw material by 0.12 volume % 48
Figure 4.4 Load-midspan displacement curves for mortar composites at flexural tests with different (a) nano biochar at 0.04 vol.% (b) hybrid nano biochar (c) raw material at 0.12 vol.% 50
Figure 4.5 Flexural fracture energy of mortar mixtures with (a) different volume of nano biochar (b) different combinations of apricot kernel shell nano biochar and sewage sludge nano biochar (c) different raw material by 0.12 volume %..... 52
Figure 4.6 Compressive strength of mortar mixtures with (a) different volume of nano biochar (b) different combinations of apricot kernel shell nano biochar and sewage sludge nano biochar (c) different raw material by 0.12 volume % 55
Figure 4.7 Load-displacement profile for mortar composites with different (a) nano biochar at 0.04 vol.% (b) hybrid nano biochar (c) raw material at 0.12 vol.% from compression tests 57
Figure 4.8 Compression fracture energy of mortar mixtures with (a) different volume of nano biochar (b) different combinations of apricot kernel shell nano biochar and sewage sludge nano biochar (c) different raw material by 0.12 volume %..... 59
Figure 4.9 SEM-EDS micrograph of mortar with apricot kernel shell biochar..... 62
Figure 4.10 Divert crack propagation in mortar matrix 63

Figure 4.11 (a) SEM image of biochar (b) SEM zoom to the square window (c) SEM-EDS micrograph of deposition of hydration products inside the pores of biochar in mortar 65

LIST OF TABLES

Page

Table 2.1 Thermochemical conversion techniques (Amalina et al., 2022; Yaashikaa, Kumar, Varjani, & Saravanan, 2020) 13
Table 3.1 The properties of cement (manufacturer data) 25
Table 3.2 The superplasticizer's specifications (manufacturer data) 26
Table 3.3 Product yields of raw materials from the pyrolysis process (wt.%) 30
Table 3. 4 Ash amount of the biochar from different raw materials (wt.%) 31
Table 3.5 The densities of the samples in the mortar mix (kg/m^3) 33
Table 3.6 Ingredients of mortar mixtures (kg/m^3) 34
Table 3.7 The specifications of Shimadzu Apparatus (manufacturer data) 39
Table 4.1 Elemental composition of the samples (wt.%) 44

LIST OF SYMBOLS

C	: Carbon
kg	: Kilogram
°C	: Centigrade celcius
s	: Second
MPa	: MegaPascal
%	: Percent
h	: Hour
CO_2	: Carbondioxide
g	: Gram
µm	: Micrometer
wt	: Weight
GPa	: GigaPascal
nm	: Nanometer
m	: Meter
mm	: Millimeter
min.	: Minutes
L	: Liter
cm	: Centimeter
ml	: Milliliter
kV	: Kilovolt
mA	: Miliampere
ρ	: density
rpm	: Revolutions per minute
kN	: Kilonewton
σ_f	: Flexural strength
L	: Span between two supports
P	: Axial load
b	: Width of the sample
d	: Depth of the sample
σ_c	: Compressive strength

O	: Oxygen
Si	: Silicon
Al	: Aluminum
Fe	: Iron
Ca	: Calcium
Mg	: Magnesium
Na	: Sodium
P	: Phosphorus
N	: Nitrogen
S	: Sulphur

ABBREVIATIONS

EJ	: Exajoule (10^{18} joule)
IBI	: The International Biochar Initiative
HTC	: Hydrothermal carbonization
BATIÇİM	: Batı Anadolu Çimento Sanayi A.Ş.
SSD	: Saturated durface dry
C	: Industrial chemical sludge
M	: Industrial mixed sludge
SS	: Municipal sewage sludge
AK	: Apricot kernel shell
TS	: Turkish Standard
ASTM	: American Society for Testing and Materials
RC	: Raw industrial chemical sludge
RM	: Raw industrial mixed sludge
RSS	: Raw municipal sewage sludge
RAK	: Raw apricot kernel shell
XPS	: X-Ray photoelectron spectroscopy
SEM	: Scanning electron microscope
CM	: control mixture
BC	: Biochar
BCC	: Industrial chemical sludge biochar
BCM	: Industrial mixed sludge biochar
BCSS	: Municipal sewage sludge biochar
BCAK	: Apricot kernel shell biochar
AKSS	: Hybrid combination of apricot kernel shell biochar and municipal sewage sludge biochar
CSH	: Calcium silicate hydrate
CSAH	: Calcium silicate aluminum hydrate

CHAPTER ONE
INTRODUCTION

This chapter presents the basis of the thesis topic in detail and then outlines the structure and the main objective of the thesis.

1.1 Background

Biomass is a type of renewable energy source that encompasses non-fossil organic material derived from biological origins, ranging from microscopic algae to large trees. Biomass includes all materials derived from living organic organisms (e.g. terrestrial or aquatic plants, forest products, animal residues, food industry and municipal waste). The energy obtained from biomass is called biomass energy. Biomass, primarily composed of carbohydrates, is the only renewable source of carbon (Xie et al., 2022).

Global biomass production has been around 220 billion dry tons per year over the past ten years. The energy equivalent of this is 4,500 EJ (1 EJ = 1.055×10^{18} joules). The amount of energy potentially generated by biomass is considerable - in fact, it is estimated to be 8.3 times greater than the total global energy consumption in 2014, which was 543 EJ. However, it is important to note that the world's known oil reserves at the end of 2017 were 1.7 trillion barrels, a reserve amount that would only be able to meet 50 years of global consumption. Therefore, there is an urgent need to replace petroleum-based materials with more diverse sources. With biomass set to be the world's most important energy source for the next 50 years, research focused on biomass is crucial (Reid, Ali, & Field, 2020).

On the other hand, concrete, a popular construction material used extensively worldwide, with an annual production of over 10 billion tons, is a significant contributor to the production of approximately 7% of global carbon dioxide emissions (Andrew, 2019; Kanojia & Jain, 2017). The traditional concrete mix consists of 12% cement and 80% aggregate in weight. Around 10 billion tons of natural materials such as crushed rock, gravel and sand are required to produce concrete each year. (Kumar

Mehta, 2001). This high level of resource consumption has led to severe damage to surface vegetation and pollution of the environment (Shafigh, Jurnaat, Mahmud, & Alengaram, 2013). The development of sustainable construction materials through their use in mortar has attracted more attention due to the effects on the environment. Various industrial and agricultural wastes such as wood, expanded glass waste, Miscanthus giganteus, oil palm shells, mussel shells, palm oil clinker, and coconut shells are being utilized as alternatives to natural aggregates to reduce their use and mitigate environmental pollution (Maldonado & Olivares, 2017).

Scientists are looking for environmentally friendly and cost-effective ways to find solutions to serious problems facing the world such as global temperature, pollution and energy crises (Abhishek et al., 2022). As the negative effects of fossil fuels on climate change, human health, and greenhouse gases effects become more concerning, the use of biomass as a renewable energy source is gaining recognition and support (Tursi, 2019).

Recent researches have focused on studying the physical properties, chemical compositions, various sources of biomass suitable for conversion, as well as the output of biomass obtained through different conversion technologies (Batidzirai, Mignot, Schakel, Junginger, & Faaij, 2013; Brown, Kercher, Nguyen, Nagle, & Ball, 2006; Gupta & Kua, 2017; Lee et al., 2013; Seow et al., 2022; Xie et al., 2022). The resulting products depend on the starting material, and the method employed for processing. Pellets, briquettes, biogas, bioethanol, biodiesel, bio-oil and biochar are among the products obtained by processing biomass (Tursi, 2019).

Biochar has become of interest as a sustainable resource for various environmental applications recently. Its unique properties have made it a viable option for environmental protection and waste recycling. An effective way to improve the environment, biochar can efficiently remove both organic and inorganic pollutants from soil and water (Abhishek et al., 2022; Seow et al., 2022). Recently, the multiple functions of biochar have gained prominence, including greenhouse gas reduction through carbon sequestration, soil fertilization, pollutant immobilization, catalyst or

catalyst precursor, energy storage, and water filtration (Ahmad et al., 2012; Lehmann & Joseph, 2009).

Biochar has been used widespread in many different areas for different purposes. Biochar, a by-product of pyrolysis or gasification of biomass, has also attracted attention as a potential filler material in concrete and mortar, which are widely used in the building industry worldwide because of their profitability and desirable mechanical properties. It is suggested that by adding biochar to building materials, carbon dioxide in the atmosphere can be captured and locked in buildings, thus reducing potential greenhouse gas emissions by 25% (Gupta & Kua, 2017).

There are many studies showing evidence that when biochar is mixed into cement and concrete, physically and mechanically stronger materials are obtained (Cao, Zhang, & Wei, 2013; Cosentino, Restuccia, Ferro, & Tulliani, 2018; Cuthbertson, Berardi, Briens, & Berruti, 2019; Falliano et al., 2020; Gupta & Kua, 2017; Gupta, Kua, & Koh, 2018a; Gupta, Kua, & Pang, 2018c; Khushnood et al., 2016; Restuccia & Ferro, 2016, 2018). The most important factor affecting the properties of biochar is the type of feedstock used. For this reason, in many studies, comparisons are made using many different biomass raw materials. There is not yet an ideal mixing ratio used in cement mixtures due to the fact that many parameters in biochar production influence the properties of the end product. Moreover, the cementitious matrix's interaction with biochar is altered due to the different processes that biochar undergoes, such as wetting, grinding, and screening, prior to its addition to cement (Sirico et al., 2020). Thus, stated that nanoparticles added to the cement composite can contribute to strength development (Kawashima, Hou, Corr, & Shah, 2013). The investigation of biochar has become a wide-ranging research area that encompasses various aspects, including raw materials, processes, ambient temperatures, products, and diverse application fields (Ramanayaka et al., 2020).

1.2 Objective

The goal of this thesis was to explore how the micro- or nano-sized biochar particles as an additive would affect both the workability and mechanical characteristics of mortar (flow, compressive strength, flexural strength, and fracture energies). For this purpose, biochar was produced from industrial and municipal wastewater sludge and lignocellulosic biomass (apricot kernel shell). Because there is currently a research gap regarding the use of biochar particles with nanoscale dimensions as an additive, as well as the utilization of biochar derived from industrial sewage sludge as an additive for mortar. Furthermore, there has been no comparative investigation to determine the effects of biomass types and waste, as well as their respective biochars, on the properties of mortar. The most important reason for choosing these wastes as a biochar raw material is that Turkey with 84 million populations is an agricultural and industrial-based country and generates a vast amount of agricultural, industrial, and municipal waste per year. The average capacity of Izmir Cigli Municipal Wastewater Treatment Plant is 604.800 m^3/day (Izmir Water and Sewerage Administration General Directorate, 2022). The water is treated in the Izmir Cigli Ataturk Organized Industrial Zone Waste Water Treatment Plant of capacity 21.000 m^3/ day (Izmir Ataturk Organized Industrial Zone, 2022). Turkey is also the world's leader apricot producer in terms of annual fresh and dried fruit yield. According to the Turkish Grain Board, 833,000 tons of fresh apricots were produced in 2020 (Turkish Grain Board, 2022). Biochar was produced by a slow pyrolysis at 500 °C and then the biochar was reduced to a nano size using a ball-milling method, and various volumes of the nano-sized biochar were added into the cement mortar. In order to understand the impact of nano biocar on the workability and mechanical characteristics of mortar, a series of mechanical tests were carried out, and the obtained results were analyzed and interpreted.

1.3 Organization of the Research

There are five main sections in the thesis. The first section, introduction, explains the basis of the thesis study in detail and the main objective of the thesis. The second

section presents fundamental information on biochar such as its properties, production methods, usage areas, and the effects of biochar on mechanical properties of mortar including the literature review. The third section explains the research methodology and materials used. The fourth section presents the experimental results and discussion, and the last section summarizes the results and outlines future plans.

CHAPTER TWO
LITERATURE REVIEW

In this section, the definition, properties, production methods and application areas of the biochar are summarized. In addition, literature studies showing how biochar affects the mechanical characteristics of the mortar such as compressive and flexural strengths and energy when added to the mortar are presented.

2.1 Properties of Biochar

The International Biochar Initiative (IBI, 2015) defines biochar as "a solid material produced from the thermochemical conversion of biomass in an oxygen-limited environment". When biomass is thermochemically converted in an oxygen-deficient or oxygen-free atmosphere, biochar, a highly porous, dark-colored carbon compound, is produced (Carvalho et al., 2022).

Using biochar dates back to ancient times. Lehmann (2009) indicated that ancient Amazonian civilizations in South America used a carbonaceous material like biochar to increase soil fertility in a human-made soil mixture called "terra preta". These soils, called Terra Preta, have a higher carbon content (150 g C/kg) as compared to soils in other nearby lands (20-30 g C/kg) (Glaser, Lehmann, & Zech, 2002). Even after many centuries, the enduring high carbon content observed in these abandoned soils serves as evidence for the long-lasting carbon stability, soil fertility, and sustainable nature inherent in organic matter. Because of the structural similarity of the organic matter in terra preta, Glaser, Balashov, Haumaier, Guggenberger, & Zech (2000) proposed the idea that the source of this efficiency could be "biochar", a concept coined by (Smith, 1980).

Similar substances rich in carbon have been used for centuries. For example, Hydrochar is an organic material that shares similarities with biochar, but distinguishes itself in terms of carbon stability and manufacturing techniques (Libra et al., 2011). Biochar can also have different characteristics within itself. Organic biomass such as

forest residues, agricultural waste, domestic solid waste, animal manure, and animal waste forms the raw material of biochar (Xie et al., 2022). Depending on the raw material used, the method applied, the temperature situation, residence time, heating rate, reactor type and other factors before or after the process, the biochar product acquires different morphological features such as the release of volatiles, pure carbon content, pore size and distribution. Therefore, defining the exact chemical composition of biochar is difficult (Tursi, 2019; Lehmann & Joseph, 2009). Figure 2.1 illustrates the biochar's structure such as its complexity, chemical, and physical composition.

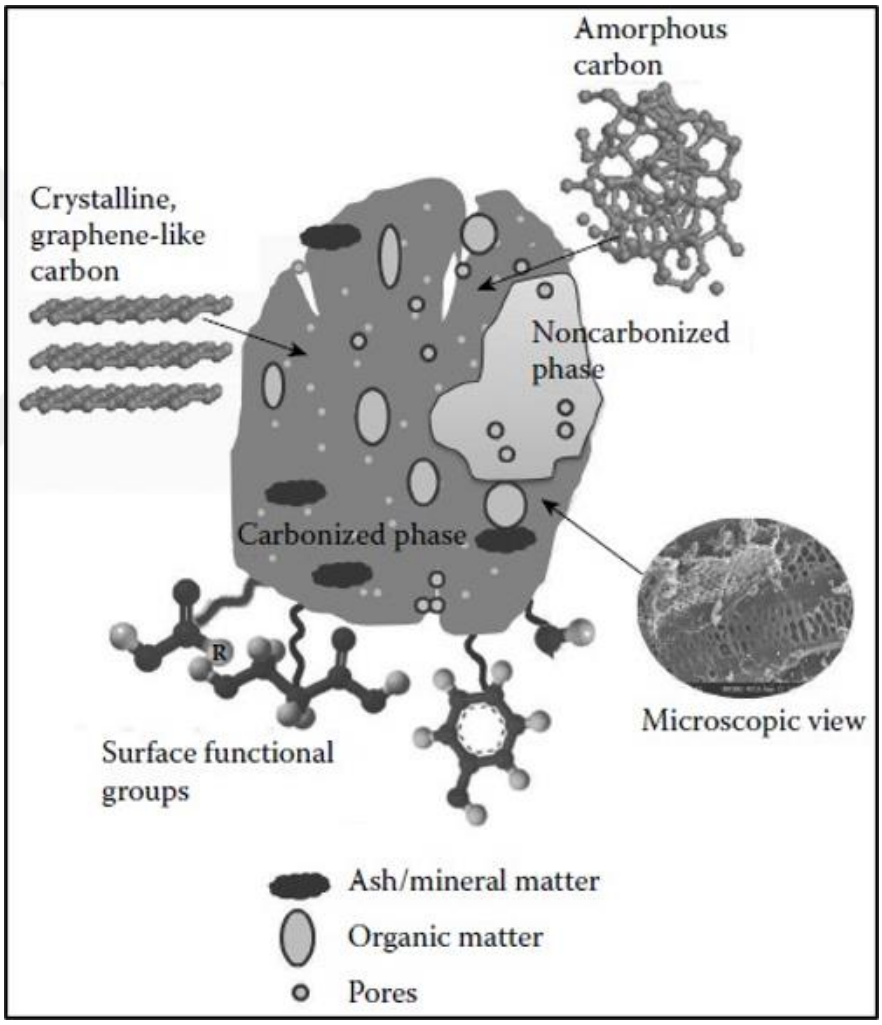


Figure 2.1 Schematic representation of biochar structure (Ok, Uchimiya, Chang, & Bolan, 2015)

Inorganic components of biochar can also include minerals including calcium, magnesium, potassium, and inorganic carbonates. However, the majority of the carbon

in biochar comes from its organic structure. The temperature required to create biochar is insufficient to create graphite, which is distinguished by the regular and aligned arrangement of aromatic rings. Consequently, depending on the kind of raw material utilized, the resulting biochar has an uneven distribution of carbon, oxygen, and hydrogen. Differently, despite having a substantial carbon content, biochar is not fully carbonized, and it can also contain some non-carbonized phases (Lehmann & Joseph 2009; Ok et al., 2015).

2.2 Production Methods of Biochar

Recently, organic waste material called biomass has been used to generate energy using various techniques such as physical, chemical, biological and thermochemical processes (Diaz-Montano, 2022). Biomass, raw material for biochar, is a complex solid with biological, organic or inorganic components. Biomass, which is classified into two groups as woody and non-woody, differs in terms of moisture, void, density and heat values. Industrial, animal, and agricultural solid wastes are considered non-woody biomass, whereas wood residues and forest residues are considered woody biomass (Tripathi, Sahu, & Ganesan, 2016). Behazin et al. (2016) pointed out that the conversion efficiency of biochemical processes is limited because they cannot process all components of biomass, whereas thermochemical processes are able to degrade all components. Therefore, thermochemical conversion methods are widely used to obtain biochar under optimal environmental conditions such as temperature ranges and residence times. Pyrolysis, flash carbonization, gasification, torrefaction, and hydrothermal carbonization are the main thermochemical conversion techniques for biomass (Carvalho et al., 2022; Pang, 2019).

2.2.1 Pyrolysis

There are many thermochemical conversion methods, but pyrolysis has gained popularity due to the conversion of biomass into a significant amount of by-products such as syngas (non-condensable), bio-oil (condensable), and a solid (biochar) (Tripathi et al., 2016). Pyrolysis is the partly combustion-based thermal breakdown of

biomass at temperatures between 250 and 900 °C without the presence of oxygen (Cha et al., 2016; Jin et al., 2016; J. Wang & Wang, 2019). Depending on the rate of heating and the amount of time needed to complete, the pyrolysis process can be categorized as slow, quick, or flash pyrolysis (Kan, Strezov, & Evans, 2016).

2.2.1.1 Slow Pyrolysis

Biomass can be heated without oxygen to produce biochar using a process referred to as "slow pyrolysis". The process usually lasts from a few seconds to several days, and is carried out at low heating rates, which range from 0.1 to 0.8 °C per second, in order to maximize the amount of biochar produced (Roy & Dias, 2017).

2.2.1.2 Fast Pyrolysis

The process of fast pyrolysis is characterized by high temperatures that cause rapid decomposition of biomass. This process is characterized by high heating rates, typically ranging between 10 and 200 °C/s, and short vapor residence times (less than 2 seconds), which reduce the subsequent breakdown of pyrolysis byproducts. The process produces a sizable volume of bio-oil as its main by-product while operating at medium to high temperatures (between 500 and 1000 ºC) without oxygen (Bruun, Ambus, Egsgaard, & Hauggaard-Nielsen, 2012).

2.2.1.3 Flash Pyrolysis

Flash pyrolysis is a rapid heating technique with exceptionally high heating rates (>1000 °C/s), high temperatures (900-1300 °C), and short residence times (0.1-1 s). This method is also known as very fast pyrolysis and is used to maximize the yield of bio-oil from biomass (Li, Rowbotham, Greenwell, & Dyer, 2013).

Several parameters associated with the pyrolysis process, including temperature, residence time, heating rate, and biomass composition, influence the properties of biochar (Tomczyk, Sokolowska, & Boguta, 2020). Higher yields of biochar can result

from the utilization of biomass with a high lignin and ash content and large particle size (Zhang, Zhu, Shen, & Liu, 2019). Increasing pyrolysis temperature decreases the yield of biochar and acidic functional groups while the relative carbon content increases but the hydrogen and oxygen content decreases (Cha et al., 2016). Furthermore, the relative ash content of the biochar increases due to pyrolyzing at higher temperatures (Suliman et al., 2016). As the temperature and residence time during pyrolysis increase, the resulting biochar tends to exhibit higher surface area and porosity. This is primarily because the release of volatile compounds during pyrolysis creates pores within the biochar structure, leading to an increase in surface area and porosity. The collapse of the porous structure, caused by excessively high temperatures and extended residence times, can result in a reduction in surface area of the biochar (Ayiania et al., 2019). Figure 2.2 depicts the development of the biochar structure in pyrolysis process.

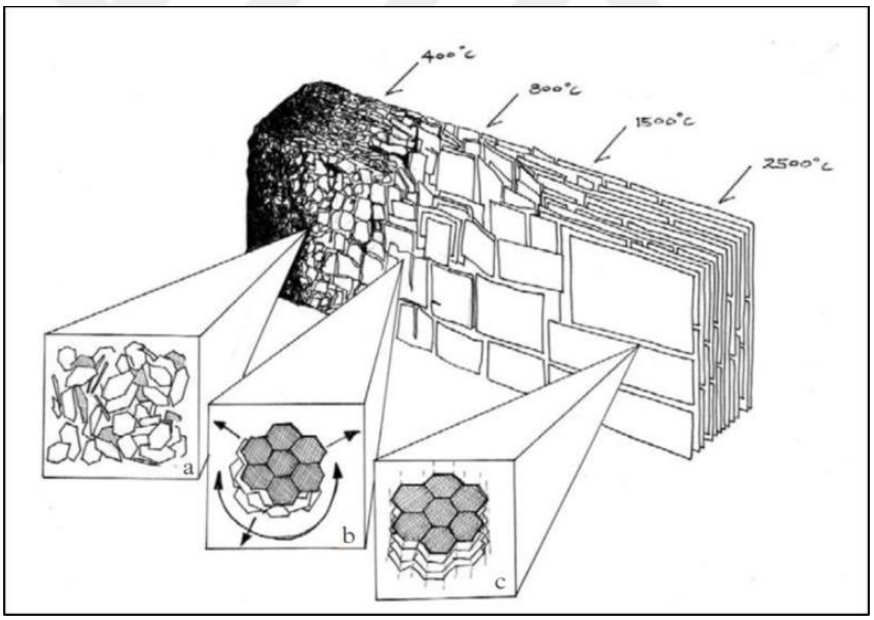


Figure 2.2 Biochar structure development during pyrolysis (Lehmann & Joseph, 2009)

Both the carbon content and the specific surface area of the product increase at higher pyrolysis temperatures (Zhao et al., 2018). In the pyrolysis process, the decrease in biochar efficiency can be attributed to two factors: 1) the easy removal of volatile

gases from the biomass at elevated temperatures, 2) the reduced carbon deposition due to the short residence time (Wang, Jiang, Zhang, & Yuan, 2020).

2.2.2 Torrefaction

Torrefaction is a technique that uses a mild pyrolysis reaction to produce biochar. This technique is conducted at relatively low temperatures, typically ranging from 200 to 300 °C, in an oxygen-free atmosphere. The residence times for this method are typically long (Krysanova, Krylova, Kulikova, Kulikov, & Rusakova, 2022). Torrefaction is also a pyrolysis method that is attracting attention for its ability to easily grind biomass and eliminate the problems encountered previously (Weber & Quicker, 2018). The torrefaction process involves minimal chemical reactions and releases only a small number of volatile compounds, resulting in increased biomass calorific value and carbon accumulation, thus leading to high productivity of the resulting biochar products (Barskov et al., 2019).

2.2.3 Hydrothermal Carbonization

Wet torrefaction, known as hydrothermal carbonization (HTC), is a process that occurs in water at high pressures (2-10 MPa) and high temperatures (18-250 °C) (Mumme et al., 2011). In the hydrothermal carbonization process, water plays a crucial role as it initiates various chemical reactions such as hydrolysis, decarboxylation, polymerization, and eventually results in the formation of char (Wang, Chang, & Li, 2019). HTC products include hydrochar, an aqueous liquid fraction (mainly organic acids, sugars, and inorganic salts), and gases (mainly carbon dioxide) (Wilk & Magdziarz, 2017). Hydrochar obtained from hydrothermal carbonization is characterized as being hydrophobic, which means it has a low affinity to water and can be easily removed (Khan et al., 2019). Wet biomass without drying can be used as feedstock in HTC (Antero, Alves, Oliveria, Ojala, & Brum, 2020; Kruse & Dahmen, 2018).

2.2.4 Gasification

In contrast to pyrolysis, gasification is characterized by combustion at temperatures of 700-1000 °C, using gasification agents such as air, pure oxygen and steam (Benedetti, Patuzzi, & Baratieri, 2018; Wang et al., 2020). Gasification, similar to fast pyrolysis, is a method that reduces product efficiency because it occurs at high temperatures, reduces the amount of carbon accumulated, and increases the equivalence ratio, which is defined as actual air–fuel to stoichiometric air–fuel for combustion (Carvalho et al., 2022).

2.2.5 Flash Carbonization

The process of "flash carbonization" involves heating biomass at high pressure (1-2 MPa) for a short period of time (about 30 minutes) while maintaining a temperature of 350–650 °C. The process has a conversion efficiency of around 40%, which decreases as pressure increases. Biochar and syngas are produced in equal amounts during the process (Antal, Modhiczuki, & Paredes, 2003; Asensio, Vega, Andrade, & Covelo, 2013).

It is crucial to carefully choose an appropriate method for the biomass feedstock and to optimize the operating conditions to maximize the biochar yield (Sirico et al., 2020a). Thermochemical conversion techniques, optimum process conditions and resulting product amounts are presented in Table 2.1.

Fast pyrolysis and gasification processes produce higher amounts of gas, which triggers the production of bio-oil or syngas. Therefore, these processes tend to produce lower quantities of biochar compared to slow pyrolysis, torrefaction, flash pyrolysis, and hydrothermal carbonization methods. While the HTC process is gaining more attention because of its ability to use wet biomass and the hydrochar's biodegradability, particularly through alkyl moieties, slow pyrolysis biochar is more stable when used as a soil amendment (Malghani, Gleixner, & Trumbore, 2013).

Table 2.1 Thermochemical conversion techniques (Amalina et al., 2022; Yaashikaa, Kumar, Varjani, & Saravanan, 2020)

Technique	Temperature (°C)	Residence time	Heating rate (°C/s)	Product yield (%)		
				Biochar	Bio-oil	Syngas
Pyrolysis	300-700 (slow)	hours to days	1-10	35	30	35
	500-100 (fast)	< 2 s	10-1000	12	75	13
Torrefaction	200-300	< 2 h	-	80	-	20
Hydrothermal Carbonization (HTC)	180-300	1-16 h	< 1	50-80	5-20	2-5
Gasification	750-900	10-20 s	0.8-1	10	5	85
Flash Carbonization	300-600	< 30 min	-	37	-	-

Slow pyrolysis is often the preferred method for producing biochar due to its ability to yield larger quantities of product and also because it is less costly to operate and pre-treat the biomass (typically around 50% less than alternative techniques) (Brown et al., 2006). Biochar's characteristics are strongly influenced by the temperature at which it is produced. The temperature determines the amounts of volatile components that are released during pyrolysis and, consequently, the pore structure of the final product. Furthermore, the remaining elements and functional groups in the resulting biochar are impacted by the temperature at which organic compounds and elements evaporate (Dhyani & Bhaskar, 2018). The temperature and residence time of the biomass feedstock during the pyrolysis process have a key role in the yield properties of biochar. Liang, Gasco, Fu, Mendez, & Paz-Ferreiro (2016) conducted a study to investigate the impact of different pyrolysis temperatures (300 °C and 500 °C) on the biochar yield of pruning wastes from parks and gardens. The results showed a decrease in biochar yield from 55 wt% at 300 °C to 36 wt% at 500 °C, indicating a reduction in biochar production as the pyrolysis temperature increased. Sun, He, Pan, & Zhang (2017) studied different types of feedstock (agricultural waste, forest litter, natural plant) to examine the influence of pyrolysis temperature (300°C, 400°C, 500°C, and

600°C) and residence time (0.5, 1, 2, 4, 8, and 24 h) on the yield of biochar. The results revealed a consistent decrease in biochar yield with increasing pyrolysis temperature, reaching a relatively stable level at higher temperatures. These variations in biochar yield were directly attributed to the composition of volatile components (such as CO, CO_2, H_2, CH_4, N_2, and gaseous carbohydrates) within the biochar, while showing an inverse relationship with the fixed carbon content. At a pyrolysis temperature of 300°C, the yield of biochar exhibited a significant reduction with longer residence times, and a stabilization in yield was observed after 8 hours. Conversely, at a pyrolysis temperature of 600°C, the increase in residence time did not have a substantial effect on the yield of biochar. This phenomenon can be explained by the observation that, as the temparature increases, the effect of increasing the residence time on the total biochar yield becomes less significant. Instead, it mainly affects the surface properties and internal structure of the biochar. Therefore, the temperature ranges given for these processes vary depending on the raw material used (Carvalho et al., 2022; Dhyani & Bhaskar, 2018; Kambo & Dutta, 2015; Ramanayaka et al., 2020). Figure 2.3 presents various types of biomass and the resultant output products obtained through biochar production methods.

Weber & Quicker (2018) examined the selection of raw materials and process designs suitable for the desired properties. According to the research results, by reviewing the results of numerous experiments, it was found that of all the parameters, the processing temperature had the greatest impact on the properties of biochar, especially the high carbon content. This research shows that the temperature ranges of 200 to 400 °C is critical for producing biochar, as significant changes in biochar's properties occur within this range. However, the sensitivity of biochar to temperature changes makes it challenging to control and results in variations in the final product's characteristics.

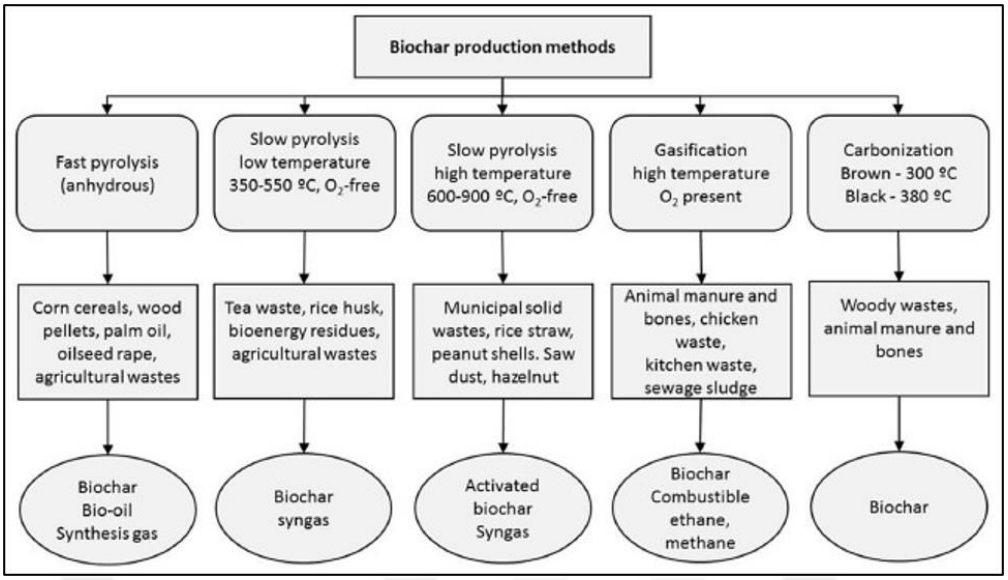


Figure 2.3 Biochar production methods with common feedstock types (Vithanage et al., 2017)

The energy requirement to achieve the pyrolysis temperature necessary for biochar production increases as the moisture content of the biomass increases. This holds true for different forms of biomass within the specified feedstock parameters. Biomass with low moisture content is more economical and preferred because it reduces the pyrolysis time (Jafri, Wong, Doshi, Yoon, & Cheah, 2018). Wang et al. (2020) stated that depending on the raw material, biochar's utility in agricultural applications varies. They also argued that there is evidence that some biochars do more harm than good and that the pyrolysis temperature and oxygen state affect the carbon state of the material obtained.

The other factor influencing the properties of biochar are the pre-treatments that the biomass undergoes before pyrolysis (Sirico et al., 2020b). Among the commonly used methods for pre-treatment of biomass; cleaning, solution immersion and particle size reduction. These processes are used to increase the yield of biochar. For example, acid treatment of small particles of pine wood can enhance the carbon content of the resulting biochar, while decreasing its oxygen and moisture levels through combustion. Due to their low binding energy, volatile components like hydrogen, nitrogen, oxygen, and sulphur evaporate during the pyrolysis of biomass. However,

biochar can have higher concentrations of minerals such as phosphorus, potassium, calcium, magnesium, and silicon (You, Ok, Tsang, Kwon, & Wang, 2018).

2.3 Biochar Usage Areas

Biochar, a substance with a high carbon content, is the environmentally friendly substance that is produced by pyrolysis of biomass. Excellent properties that make biochar suitable in a range of applications set it apart from other materials (Weber & Quicker, 2018). Figure 2.4 demonstrates the various potential uses of biochar.

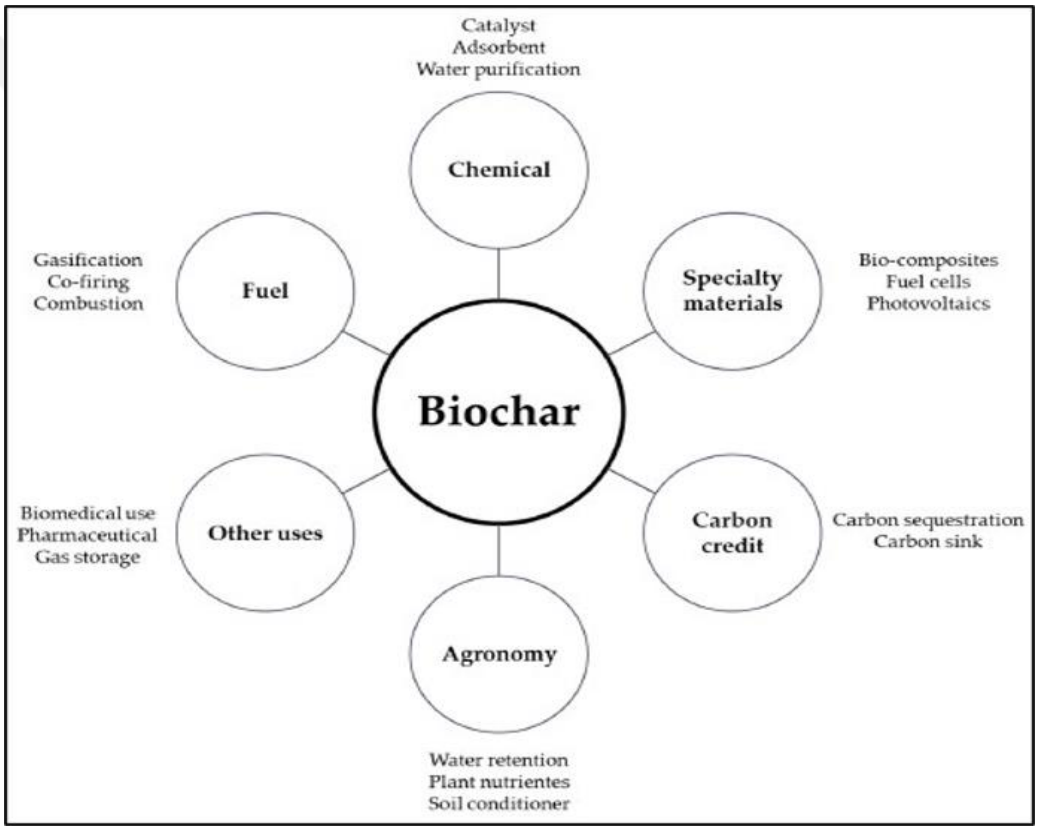


Figure 2.4 Biochar application areas (Carvalho et al., 2022)

Figure 2.5 illustrates some of the potential benefits of using biochar in farming and forestry systems. It has been demonstrated that adding biochar to agricultural soils improves their physical characteristics, leading to considerable gains in productivity and crop yields.

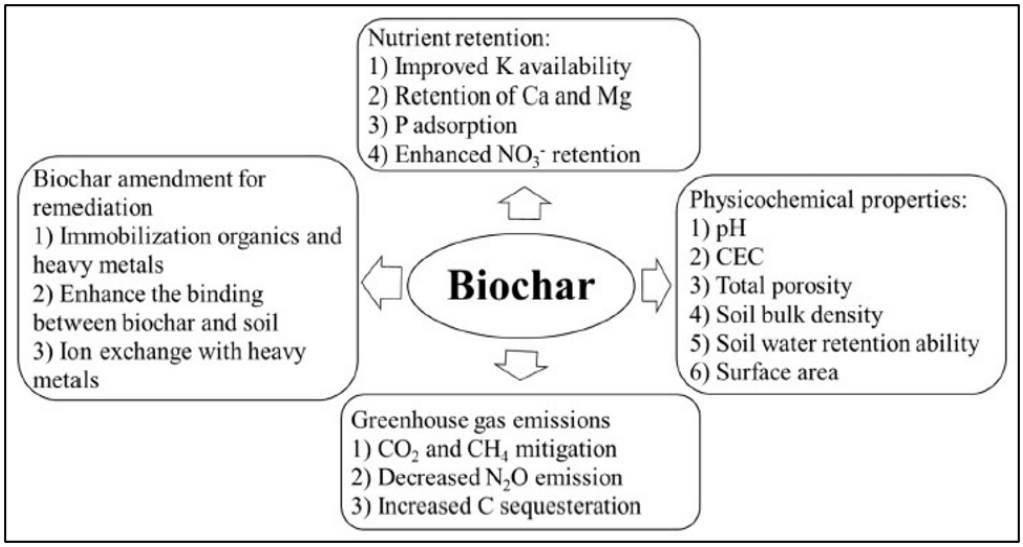


Figure 2.5 Benefits of biochar in farming and forestry systems (Wang et al., 2020)

In addition to its role in improving nutrient retention and soil fertility, biochar has potential applications as an adsorbent in water treatment systems due to its ability to detect pollutants at the nanoscale and high adsorption capacity (Abhishek et al., 2022; Pratap, Patel, Pittman, Nguyen, & Mohan, 2021). Heavy metals, which are non-degradable and have carcinogenic and harmful effects, can be removed by biochar due to its chemical and physical properties. When nutrient levels such as potassium, sodium, phosphorus, and nitrogen exceed certain limits, they can become harmful. Biochar can remove these components using various methods such as hydroxyl functional complexation, ligand exchange, electrostatic interaction, and precipitation with magnesium or calcium ions (Beckinghausen et al., 2020; Zhao et al., 2018).

Biochar has recently grown in appeal as a tool for reducing greenhouse gas emissions due to its capacity to sequester carbon in a variety of uses (Weber & Quicker, 2018). Anthropogenic emissions of carbon dioxide (CO_2) have increased by 3% worldwide since 2000, posing a threat to ecosystems due to climate change. However, biochar's ability to sequester carbon offers hope for addressing global warming. In the construction industry, incorporating biochar into cementitious building materials provides an eco-friendly alternative to energy-intensive additives such as cement and sand. In addition, studies have shown that the use of biochar can

increase the concrete's compressive and flexural strength by up to 15-20%, a 30-40% reduction in capillary water absorption and the ability to adsorb and remove heavy metals from leachate (Seow et al., 2022). Figure 2.6 illustrates the impact of biochar produced through pyrolysis on mitigating global warming. Total greenhouse gas emissions decrease as a result of the process through which carbon dioxide is removed from the atmosphere and stored in soil.

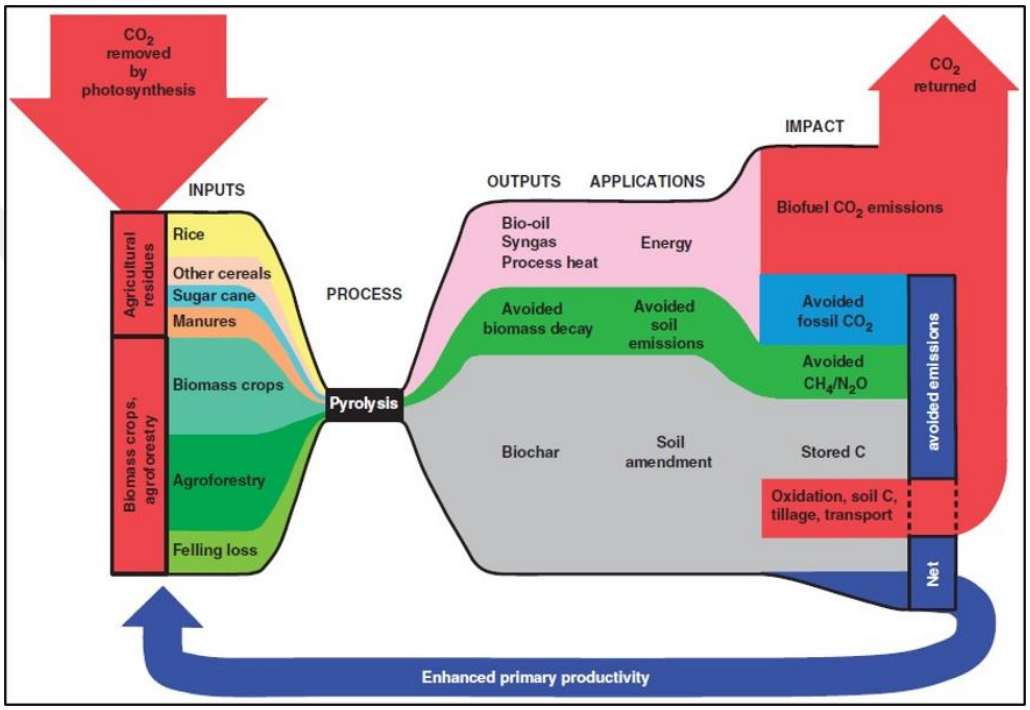


Figure 2.6 The impacts of biochar produced by pyrolysis on global climate (Woolf, Amonette, Street-Perrott, Lehmann, & Joseph, 2010)

The components shown in Figure 2.6 are colored in proportion to their relative areas. Photosynthesis is responsible for transferring CO_2 from the atmosphere to biomass. Residues from agriculture and forestry are included in biomass, which can then be pyrolyzed to produce biochar, bio-oil, and synthesis gas. Biochar has two advantages that it can act as a carbon sequestrant, storing carbon much longer than biomass that is left to decompose naturally, and as a soil conditioner. This is in contrast to bio-oil and syngas, which release CO_2 when burned for energy. Biochar has a greater potential impact on the climate as compared to bioenergy, due to its positive effect on soil fertility and reduction of greenhouse gas fluxes in the soil (Woolf et al., 2010).

The unique properties of biochar have made it a versatile material with various applications in different fields. Biochar is used as a soil supplement in agriculture to improve soil qualities, augment crop yield, improve nutrient retention, and reduce greenhouse gas emissions. Biochar is a promising adsorbent in the water treatment industry to remove various contaminants, including heavy metals, from water effectively due to its high adsorption capacity and ability to detect pollutants at the nanoscale. Biochar has also been utilized in the construction sector as a substitute or additive material to improve material properties while reducing environmental impact. Biochar can be used as a fuel or in battery storage due to its high carbon content and stability for energy production and storage. Moreover, biochar can also assist reduce air pollution by acting as a catalyst or catalyst precursor in various chemical reactions. Additionally, biochar is an effective feed supplement for livestock (Amalina et al., 2022; Iwuozor et al., 2022).

2.4 Nano Biochar Production

As the size of the biochar is reduced to the nanolength scale, the surface area increases, providing areas of surfactant, porosity, and surface functional groups (Pratap et al., 2021). Nano biochar, which is obtained by mechanically grinding biochar obtained by pyrolysis of biomass, has recently attracted a lot of attention and research. Furthermore, direct nano biochar production was achieved by flash heating, resulting in graphitic nanosheets. In order to avoid expensive precursors, high energy consumption, and sophisticated processes in the production of nanoparticles, inexpensive, environmentally friendly methods are widely preferred. The process of ball milling is depicted in Figure 2.7, which is used to break down biochar material into nanoparticles while preserving its crystal structure.

The ball milling technique is a versatile method widely used due to its ability to be applied to a wide range of materials. The size and surface properties of nano biochar particles produced through ball milling depend on various parameters, including the weight and diameter of the balls used, the speed of rotation, the ratio of ball force to mass, and the duration of milling. The kind of material used in the milling process

affects the choice of ball weight and diameter. In addition, it is considered one of the emerging parameters in this field. The literature shows that different types of balls are used for different biochar materials. For example; 30-45 g stainless steel balls for pine wood and modified rice hull materials in the grinding process; 180 g agate balls for materials from sugar cane, bamboo, pulp and walnut wood; 100 g agate balls were used for wheat straw (Li et al., 2020; Shah et al., 2015; Peterson, Jackson, Kim, & Palmquist, 2012). Although nano biochar has various applications including wastewater treatment, health applications, electrode material, supercapacitors and sensors, it has disadvantages such as high potential for agglomeration and low efficiency in practical application (Ramanayaka et al., 2020).

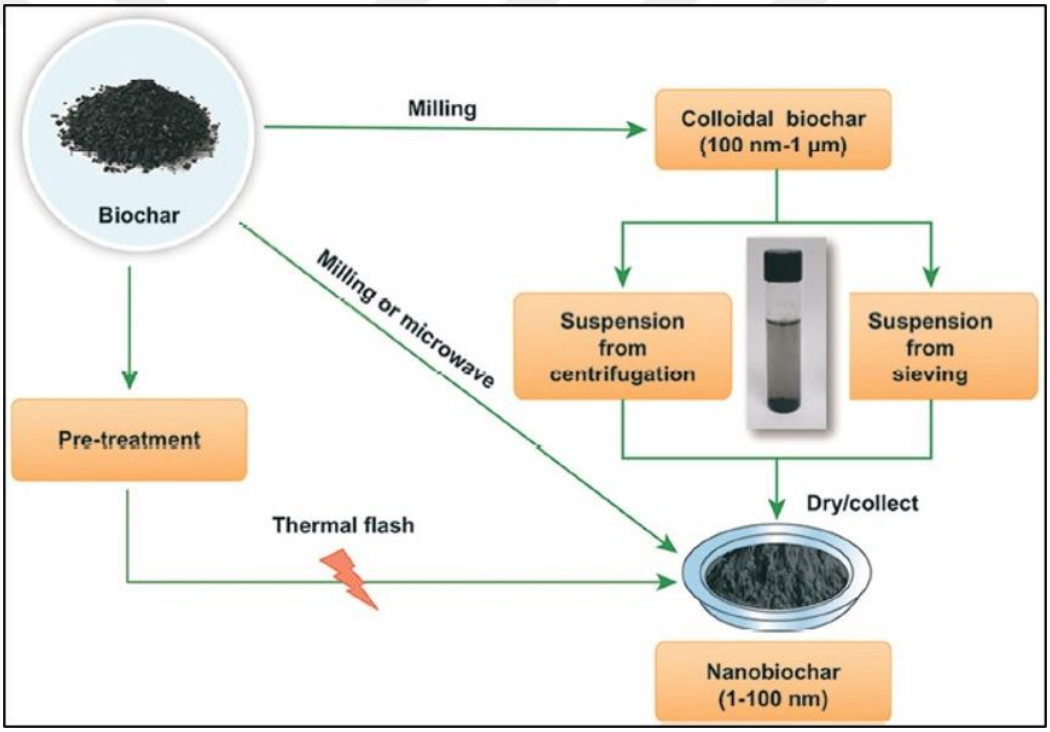


Figure 2.7 The nano biochar preparation process (Ramanayaka et al., 2020)

2.5 Effect of Biochar on Mortar or Concrete's Mechanical Properties

Numerous studies have found that biochar exhibits promising potential as an additive or cement replacement in mortar and concrete composites due to its properties, such as low thermal conductivity, reduced flammability, and superior

chemical stability (Mensah et al., 2021). In comparison to the reference, the authors demonstrated that biochar produced from various biomass feedstocks under optimum pyrolysis conditions significantly improved the mechanical qualities of mortar and concrete. In addition to biochar's potential to influence the evolution of mechanical properties of mortar composites when used in the construction industry, another benefit is its contribution to reducing global warming through carbon sequestration (Gupta & Kua, 2017).

Biochar has large surface areas and pores volume since volatile substances escape during pyrolysis. The reduction in the water-to-cement ratio during mortar preparation thanks to these pores can improve the mechanical properties of cementitious biochar composites (Gupta, Kua, & Low, 2018b).

Gupta, Kua, & Pang (2018c) added biochar with a particle size of 10.7 μm, obtained from mixed sawdust at 500 °C, to the mortar in an amount of 1% by weight. As a result of the experiment, the addition of biochar caused an increase of 16% in the compressive strength and 13% in the flexural strength of the mortar.

In order to enhance the qualities of lightweight concrete, Wu, Liu, Zhang, Lu, & Ma (2018) investigated the impacts of adding peach and apricot peel biochar to the cement mix. The concrete's mechanical and physical qualities were improved, according to the authors. The concrete's density, water absorption, and open porosity were all decreased while its overall porosity was increased by the carbonized peach and apricot peels. Mechanically, it was found that the highest results were for the carbonized apricot peel. The determined values for the carbonized apricot peel and the recovery rates relative to the non-carbonized slider skin are as follows: compressive strength (38.8 MPa, 44.2% improvement), splitting strength (3.54 MPa, 55.3%), flexural strength (5.49 MPa, 54.6%) and Young's modulus (15.1 GPa, 42.5%).

Akhtar & Sarmah (2018) substituted 0.1% of the total cement volume with three different biochars made from rice husk, paper mill waste, and poultry litter. The flexural strength of cement mortar increased by 20% when 0.1% poultry waste and

0.1% rice husk biochar were applied separately, and the splitting strength was also improved by 0.1% rice husk biochar, according to the authors. However, only a slight improvement in strength was observed when using paper mill biochar and pulp sludge biochar. On the other hand, Mrad & Chehab (2019) investigated the compressive strength and microstructural characteristics of a mortar made with municipal solid waste and biochar that had 10-45% included as a partial replacement for sand. The findings indicated that the substitution of sand with biochar in the mortar led to a reduction in compressive strength, regardless of whether the hardening process occurred in air or water. This decrease could be attributed to the porous characteristics of biochar and its ability to absorb a significant amount of water.

Han (2020) investigated if it was feasible to substitute 1-3% of the mortar cement with peanut biochar. In comparison to the control, the inclusion of 3% biochar increased compressive strength by 22%.

Qin, Pang, Tan, & Bao (2021) conducted a study that demonstrated the positive impact of incorporating biochar derived from eucalyptus synthetic plywood panels into permeable concrete samples. The inclusion of biochar resulted in improvements in both compressive strength and splitting tensile strength, ranging from 0.0% to 6.5%. This is because little amount of biochar triggers cement hydration, and since more hydration products are produced with biochar, the strength of pervious concrete is increased.

The use of raw, pyrolyzed (biochar), and burned (bioash) sewage waste as substitutes for cement was studied by Roychand et al. (2021). Of all, biochar performed the best as a cement replacement material, providing ~278% strength improvement and ~87% reduction in overall porosity with the addition of 10% biochar.

In order to evaluate the performance of biochar-based mortars or cement pastes under fire conditions, Navaratnam, Wijaya, Rajeev, Mendis, & Nguyen (2021) examined the changes in compressive strength of the mortar composites after subjecting them to high temperatures (200 °C, 450 °C, and 700 °C). This study

revealed that addition of biochar to the mortar, at a dosage of 5% by weight of cement, resulted in an increase in compressive strength at room temperature and a decrease in strength loss at higher temperatures, indicating biochar's potential for enhancing the fire resistance of the mortar.

Numerous studies have suggested using nanoparticles to create cement-based materials with superior properties in the construction industry. These nanoparticles would have characteristics like a large surface area, high functional density, extraordinary surface effect, and high elongation resistance (Al-Hagri & Döndüren, 2022; Lee, Mahendra, & Alvarez, 2010; Mohajerani et al., 2019; Norhasri, Hamidah, & Fadzil, 2017; Shilar, Ganachari, & Patil, 2022; Wang, Zhang, & Gao, 2018). By filling the micropores in the structure of the cement paste, nanoparticles enhance the strength and mechanical qualities of cement mortar (Al-Rifaie & Ahmed, 2016; Ramakrishna & Sundararajan, 2019).

Ahmad, Khushnood, Jagdale, Tulliani, & Ferro (2015) investigated how pyrolyzing bamboo to produce biochar affected the mechanical properties of cement paste, such as compressive and flexural strength. The biochar was added to the sludge paste in the form of carbonized microparticles [1-2 μm] in an amount of 0.05-0.20% by weight. At 0.08% by weight, bamboo particles were shown to improve compressive strength by 30% and flexural strength by 20%.

Sirico et al. (2020a) aimed to determine the optimal biochar content of micro-nano biochar from forest chips by gasification at 700 ºC. The authors added the biochar to the cement mortar in different proportions. Mechanical test results showed that adding biochar in the appropriate quantity enhances concrete's flexural strength and results in more ductile behavior in cementitious composites. It was found that the optimum biochar filler ratio to add to the cement was 2%, and the filler added less than this ratio had no effect. Addition of less than 2% biochar leads to multiple fractures. More than 2.5% of the additives for biochar have to be modified. The measurements showed that in 7 days an improvement in flexural strength of more than 15% and an improvement in fracture energy of more than 150% was achieved.

Restuccia & Ferro (2016) utilized hazelnut shells and coffee powder as raw materials in their study. They observed that by incorporating 1% by weight of biochar into the mortar, the 7-day compressive strength improved by up to 30% compared to the control mortar. Additionally, they discovered that adding 0.5 wt% hazelnut shell nano biochar (particle size distribution between 300 nm to 15 μm) significantly increased both compressive and flexural strength compared to the control mortar by 44.5% and 64%, respectively.

Khushnood et al. (2016) incorporated biochar from peanut and hazelnut shells into mortar by reducing its size to nano dimensions. The studies revealed that 1% biochar added to cement paste increased the mortar's flexural strength and toughness, creating high-performance cement composites.

The chemically inert, non-degradable, and carbon-rich nature of biochar presents opportunities for improving mechanical characteristics of mortar composites and also mitigating net greenhouse gas emissions by sequestering carbon. According to Roberts, Gloy, Joseph, Scott, & Lehmann (2010), carbon capture and storage using biochar feedstock can result in reductions of greenhouse gas emissions of 62% to 66%.

Cuthbertson et al. (2019) studied that the incorporation of biochar from residual biomass from bioethanol production at a biochar concentration of 15% by weight can lead to a reduction in concrete density. By forming pore networks inside the substance, this addition can further increase the sound absorption coefficient of concrete over the frequency range of 200-2000 Hz. Additionally, at a biochar concentration of 2% by weight, the concrete's thermal conductivity is reduced the most.

Praneeth, Saavedra, Zeng, Dubey, & Sarmah (2021) replaced the sand component of the mortar with biochar derived from poultry litter. Substituting 40% of the sand with biochar resulted in a 20% reduction in CO_2 emissions compared to the control mortar.

CHAPTER THREE

MATERIALS AND METHOD

All materials and methods used in this study have been specified in this section.

3.1 Materials

3.1.1 Cement and Sand

For this research, CEM II / B-M (L-W) 42.5R cement supplied by Batı Anadolu Cement Industry Co. Ltd. (BATIÇİM) was utilized as a binder. The cement was stored in plastic containers to avoid moisture-related issues. Table 3.1 shows the properties of the binder.

The BATIBETON Company supplied fine aggregates comprised of crushed limestone with a maximum particle size of 5mm. Under saturated surface dry (SSD) conditions, the aggregates had a specific gravity of 2630 kg/m^3, a moisture content of 0.17%, and a water absorption rate of 1.87%.

Table 3.1 The properties of cement (manufacturer data)

Chemical analysis (%)		**Physical properties**	
CaO	53.1	Specific gravity (kg/m^3)	2970
SiO_2	24.7	Specific surface area (m^2/kg)	460.7
Al_2O_3	8.8	Compressive strength (MPa)	
FCaO	3.21	2 days	25.2
Fe_2O_3	2.78	28 days	52.1
SO_3	2.74	Setting time (min)	
MgO	2.18	Setting time (initial)	175
K_2O	0.95	Setting time (final)	225
Na_2O	0.17		
Cl-	0.09		
Loss	1.36		

3.1.2 Water

Distilled water was used in mixing processes. Millipore ultrapure water device, electrodeionization (E.D.I) module (Elix ® 5 Water System, was used to produce the distilled water.

3.1.3 Superplasticizer

Sika Viscocrete Hi-Tech30 was employed as a superplasticizer in the mortar mixtures to facilitate the workability during the mixing process. This superplasticizer was provided by Sika Construction Chemicals Co. and its specifications are given in Table 3.2.

Table 3.2 The superplasticizer's specifications (manufacturer data)

Chemical base	Modified polycarboxylates based polymer
Density	1.07-1.11 kg/L, 20 °C
pH value	3 - 7
Freezing point	-9 °C
Chloride ion content soluble in water % w/w	Max. 0.1%, Chloride-free
Equivalent sodium oxide as % Na_2O	Max. 0.4%

3.1.4 Biochar Production

Chemical sludge (C) and mixed sludge (M) (chemical and biological) supplied by Wastewater Treatment Units of Cigli Ataturk Organized Industrial Zone, sewage sludge (SS) supplied by Municipal Wastewater Treatment Plant in Cigli and apricot kernel shell (AK) taken from a local production factory of apricot juice in Malatya were used to produce biochar. The wet chemical sludge was taken from the treatment pool and was air-dried for two weeks (Figure 3.1a-b-c). The mixed sludge was taken dry from the drying pool (Figure 3.1d). The municipal sewage sludge and the apricot kernel shell were taken dry (Figure 3.1e-f).



Figure 3.1 The raw material of (a-b-c) industrial chemical sludge (d) industrial mixed sludge (e) dried municipal sewage sludge (f) dried apricot kernel shell (Personal archive, 2019)

The raw materials have undergone a thermal decomposition process called slow pyrolysis, in which the materials are heated in an oxygen-free environment. This process converted the raw materials into three forms: a solid, high-carbon residue known as biochar, synthetic fuel gas or synthesis gas, and fuel oils or bio-oils (Jin et al., 2016). The pyrolysis experimental setup is represented in Figure 3.2. Figure 3.2a depicts the stainless steel vertical fixed bed reactor that Kantarli & Yanik (2009) utilized. The reactor has a height of 21 cm and a diameter of 6 cm.

In the experimental process, the raw sample was subjected to heat treatment in a reactor, as shown in Figure 3.2a. The temperature was raised progressively until it reached 500 °C and then held there for an hour at a rate of 10 °C/min. The temperature was monitored and controlled using a thermocouple, as shown in Figure 3.2c. A nitrogen gas flow of 50 ml/min was used to remove volatile gases and maintain an oxygen-free environment in the reactor (Figure 3.2b). The volatile gases swept away by nitrogen gas were condensed into liquid products containing liquid and organic phase in ice-cooled vessels. At the end of each experiment, the weights of the biochar and liquid products were measured, the gas fraction was determined using the difference and the pyrolysis efficiency was calculated (Figure 3.2d-e).

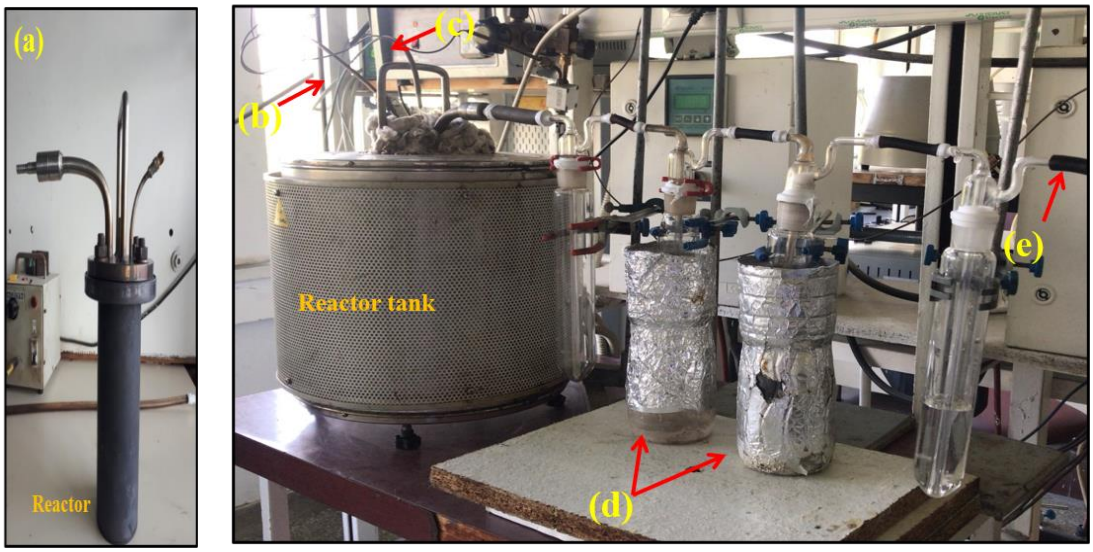


Figure 3.2 Pyrolysis experiment: (a) vertical reactor (b) nitrogen gas (c) thermocouple (d) liquid collection flasks (e) gas products (Personal archive, 2019)

The raw materials and the produced biochar by pyrolysis process were presented in Figure 3.3.



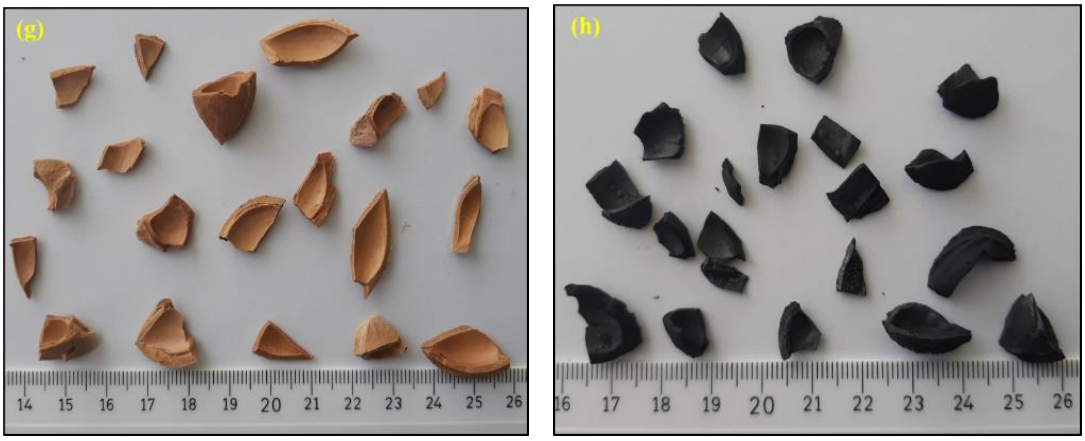


Figure 3.3 Raw material and produced biochar (a) industrial chemical sludge (b) industrial chemical sludge biochar (c) industrial mixed sludge (d) industrial mixed sludge biochar (e) municipal sewage sludge (f) municipal sewage sludge biochar (g) apricot kernel shell (h) apricot kernel shell biochar (Personal archive, 2019)

The product yields of pyrolysis process was presented in Table 3.3. The highest biochar yields were obtained from industrial chemical and mixed sludges which is attributed to their high ash content (see Table 3.4).

Table 3.3 Product yields of raw materials from the pyrolysis process (wt.%)

Name code	Name description	Biochar	Liquid	Gas
RC	The raw industrial chemical sludge	67.62	22.85	9.54
RM	The raw industrial mixed sludge	69.01	21.36	9.63
RSS	The raw municipal sewage sludge	55.47	34.17	10.37
RAK	The raw apricot kernel shell	28.79	55.43	15.78

The ash content of the biochar was calculated in accordance with ASTM D3174-04 (2010) and then calculated according to equation 3.1. The ash content of the produced biochar was shown in Table 3.4.

$$Ash\ content\ [\%] = \frac{weight\ of\ ash}{dry\ weight\ of\ biochar}\ \text{x}\ 100 \qquad (3.1)$$

Table 3. 4 Ash amount of the biochar from different raw materials (wt.%)

Name code	Name description	Ash amount
BCC	Biochar obtained from industrial chemical sludge	88.3
BCM	Biochar obtained from industrial mixed sludge	89.28
BCSS	Biochar obtained from sewage sludge	51.24
BCAK	Biochar obtained from apricot kernel shell	1.09

Before mixing into mortar, the raw samples, and the biochars obtained from the pyrolysis process were ground into nano-size (<500 nm) by using Fritsch Premium Line Pulverisette 7 (Cosentino et al., 2018).

3.2 Methods

3.2.1 Characterization of Raw Material and Nano Biochar

The elemental ingredients of the samples were examined using the Thermo Scientific K-Alpha equipment, a high-sensitivity X-ray Photoelectron Spectroscopy (XPS) tool.

Morphological analysis, particle size determination, surface structure examination, and elemental analysis of the samples were carried out using COXEM EM-30 Plus scanning electron microscope (SEM) device operating at 20 kV acceleration potential for raw sample, nano biochar and ZEISS GeminiSEM 560 device for the cured mortar. Prior to imaging, the samples were dried and coated with gold using a sputter coater operating at a current of 60 mA. The pycnometer method depicted in Figure 3.4 was used to determine the densities of the raw materials and nano biochar.

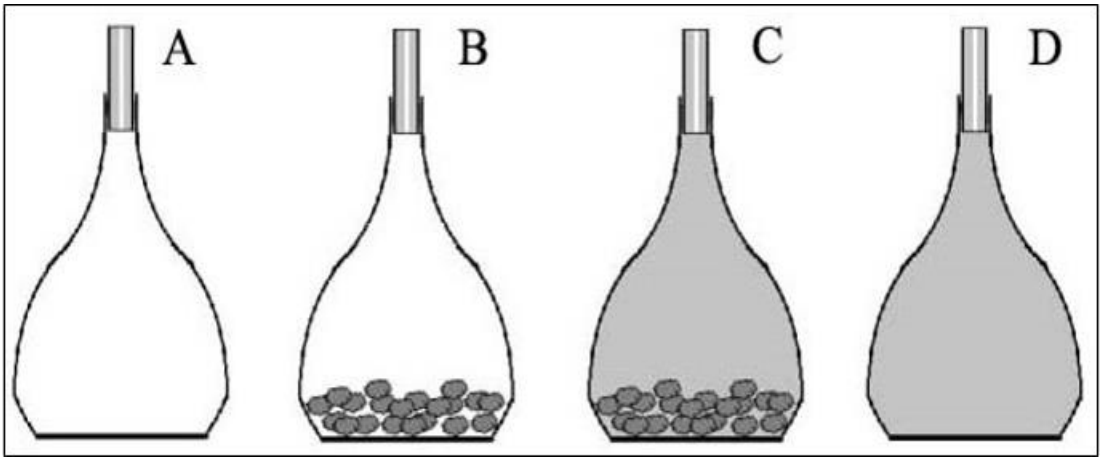


Figure 3.4 Determination of density process

The pycnometer a small balloon with a capillary corrugated glass cap placed in its mouth is used to measure the actual density of powdered materials (typically -200 μm). In this study, toluene was used for organic solvent. Firstly, the pycnometer was dried at 25 ^{o}C with the capillary head and weighed, (A). Secondly, a small amount of sample powder was put into the pycnometer and weighed, (B). Then, slowly filled the pycnometer with organic solvent and shaken intermittently to ensure that no air bubbles remained between the grains and was weighed together with the capillary head, (C). Finally, the pycnometer was emptied, filled with organic solvent at the same temperature, and weighed, (D). The density of the raw materials and biochar at the nanoscale was determined as follows:

$$Density = \frac{(B-A)}{(D-A)-(C-B)}\ x\ \rho \tag{3.2}$$

in which ρ is the density of toluene equal to 0.865 g/cm^3. Table 3.5 shows information on the samples' densities that were utilized for the experimental study.

Table 3.5 The densities of the samples in the mortar mix (kg/m^3)

Name	Industrial chemical sludge	Industrial mixed sludge	Municipal sewage sludge	Apricot kernel shell
Raw sample	2280.9	1822.9	1301.5	1319.8
Nano biochar	2321.4	2188.0	1344.9	1184.5

3.2.2 Mortar Mixture's Preparation

3.2.2.1 Mortar Mixture's Design

Based on TS 802 (2016), mortar mixes were developed to determine the effects of the produced nano biochar on the mechanical properties of the mortar by adding to the mortar in different volume percentages. The water/binder ratio was adjusted to 0.47. According to the best results obtained, a hybrid mixture of apricot kernel and sewage sludge biochar in different proportions was added to the mortar to find out the synergic effect on the mechanical properties of mortar. In order to compare the results, the raw materials were added to the mortar separately without pyrolysis at 0.12 percent by volume. As a result, a total of 26 combinations were prepared, one of which was used as a control mix (CM) not containing nanobiocar. Mix codes and proportions of mortar mixes were given in Table 3.6.

3.2.2.2 Mortar Mixing, Flow Test

Before preparing the mortar mixtures, a sequential process was followed to disperse the additives, including nano biochar, a hybrid combination of nano biochars, and nano raw materials, in a solution containing distilled water and plasticizer. This process, shown in Figure 3.5, involved the initial mixing of water and plasticizer in a glass beaker using a magnetic stirrer at 1500 rpm for 5 minutes (a). Subsequently, the required amount of powdered additive material was added to the solution, which was further mixed for 30 minutes (b). To ensure proper homogenization and prevent aggregation of nano biochar particles, the mixture underwent sonication for 30 minutes in an ultrasonic bath (c). Following this, the mixture was immediately subjected to additional stirring with a magnetic stirrer at 1500 rpm for 30 minutes (d).

Table 3.6 Ingredients of mortar mixtures (kg/m³)

Mix code	Mix description	Cement (kg)	Sand (kg)	Water (kg)	Biochar (kg)	Superplasticizer (kg)
CM	Control mixture-mortar without biochar	485	1472	253	0	2.4
BCC04	Mortar with 0.04 vol% BCC	485	1471	253	0.93	2.4
BCC06	Mortar with 0.06 vol% BCC	485	1470	253	1.39	2.4
BCC12	Mortar with 0.12 vol% BCC	485	1469	253	2.77	2.4
BCC15	Mortar with 0.15 vol% BCC	485	1468	253	3.48	2.4
BCM04	Mortar with 0.04 vol% BCM	485	1471	253	0.88	2.4
BCM06	Mortar with 0.06 vol% BCM	485	1470	253	1.32	2.4
BCM12	Mortar with 0.12 vol% BCM	485	1469	253	2.64	2.4
BCM15	Mortar with 0.15 vol% BCM	485	1468	253	3.30	2.4
BCSS04	Mortar with 0.04 vol% BCSS	485	1471	253	0.59	2.4
BCSS06	Mortar with 0.06 vol% BCSS	485	1470	253	0.82	2.4
BCSS12	Mortar with 0.12 vol% BCSS	485	1469	253	1.51	2.4
BCSS15	Mortar with 0.15 vol% BCSS	485	1468	253	1.86	2.4
BCAK04	Mortar with 0.04 vol% BCAK	485	1471	253	0.47	2.4
BCAK06	Mortar with 0.06 vol% BCAK	485	1470	253	0.71	2.4
BCAK12	Mortar with 0.12 vol% BCAK	485	1469	253	1.43	2.4
BCAK15	Mortar with 0.15 vol% BCAK	485	1468	253	1.79	2.4
AKSS0202	Mortar with a hybrid combination of 0.02 vol% BCAK and 0.02 vol% BCSS	485	1471	253	0.24 0.27	2.4
AKSS0402	Mortar with a hybrid combination of 0.04 vol% BCAK and 0.02 vol% BCSS	485	1470	253	0.47 0.27	2.4
AKSS0404	Mortar with a hybrid combination of 0.04 vol% BCAK and 0.04 vol% BCSS	485	1470	253	0.47 0.54	2.4
AKSS0503	Mortar with a hybrid combination of 0.05 vol% BCAK and 0.03 vol% BCSS	485	1470	253	0.59 0.40	2.4
AKSS0505	Mortar with a hybrid combination of 0.05 vol% BCAK and 0.05 vol% BCSS	485	1469	253	0.59 0.67	2.4
RC12	Mortar with 0.12 vol% RC	485	1469	253	2.74	2.4
RM12	Mortar with 0.12 vol% RM	485	1469	253	2.26	2.4
RSS12	Mortar with 0.12 vol% RSS	485	1469	253	1.56	2.4
RAK12	Mortar with 0.12 vol% RAK	485	1469	253	1.59	2.4

AKSS: Hybrid combination of apricot kernel shell biochar and sewage sludge biochar



Figure 3.5 Dispersion process (Personal archive, 2020)

After the dispersion process (as shown in Figure 3.6), the mortar mixtures were prepared in a 5-liter capacity stainless steel bowl. Initially, sand and cement were separately mixed in a dry state, ensuring thorough mixing (Figure 3.6a). Subsequently, the liquid mixture containing the additive material was added twice to the dry mixture and manually mixed each time (Figure 3.6b). Finally, the mixture was further mixed using a mortar mixer, initially at 140 rpm for 30 seconds and then at 280 rpm for an additional 150 seconds (Figure 3.6c).



Figure 3.6 Mortar mixing with 5-liter capacity mixer (Personal archive, 2020)

Mortar flow tests were performed accordance with ASTM C1437-15 (2015) prior to pouring into molds. Thus, a design that regulates the self-compacting mortar was maintained. The test apparatus, known as an Abrams cone, has a height of 60 mm, a top diameter of 70 mm, and a base diameter of 100 mm. It is open at the bottom and top (Figure 3.7). In the test procedure, attention was paid to ensure that the flow chart was wet. The cone was filled with fresh mortar by placing it in the middle of the flow

chart as in Figure 3.7a. After waiting for 30 seconds, the cone was removed and the mortar was allowed to flow. The diameter of the mortar, whose final state is shown in Figure 3.7b, was measured and recorded.

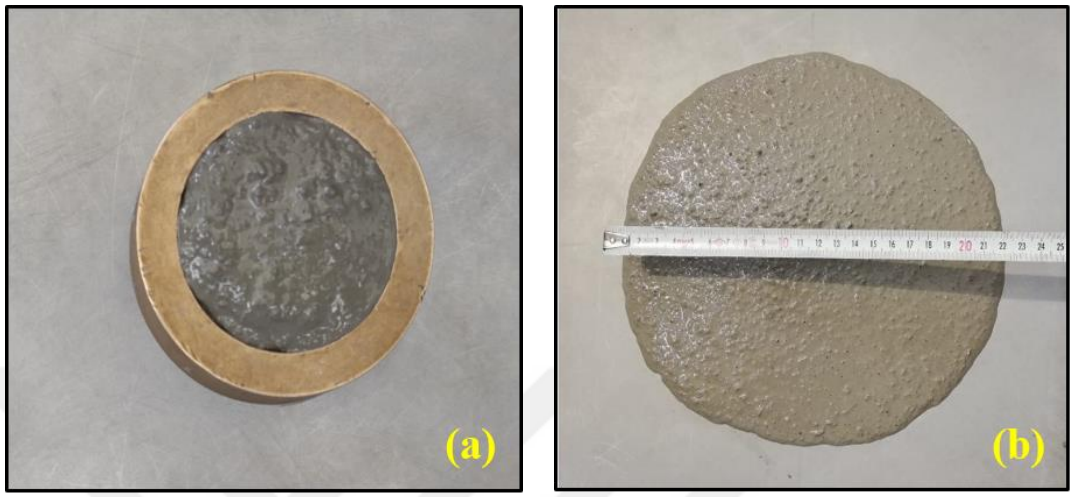


Figure 3.7 Mortar flow test (Personal archive, 2020)

3.2.3 Molding, Curing

The mortar paste was placed into prismatic moulds measuring 40 x 40 x 160 mm after the flow test and left there for 24 hours. Three prismatic blocks were obtained for each mixture. The blocks were removed from the moulds and the test surfaces were smoothed with a spatula. Thus, it is prevented from being subjected to any oblique loading during mechanical experiments (Figure 3.8).

The prepared specimens were placed in the curing tank as shown in Figure 3.9 with their names written on the surface. The samples were cured for 28 days in a water tank with the water temperature set to 20°C, and after being removed from the tank, the hardened blocks were kept in the laboratory for 7 days to reach a constant moisture content.

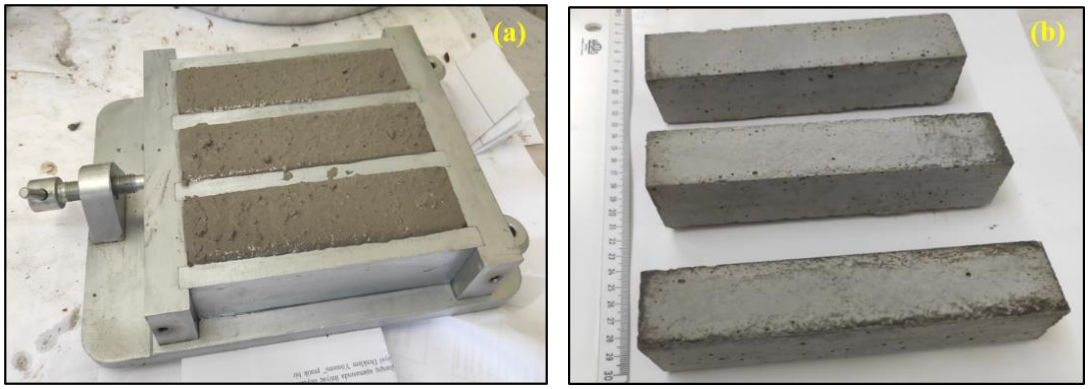


Figure 3.8 Molding (a) molds (b) specimens after 24 hours from the molds (Personal archive, 2020)



Figure 3.9 Curing tank (Personal archive, 2020)

3.2.4 Testing of the Mortar Samples

The mechanical characteristics of the mortar samples, including flexural and compressive strengths, were determined using the 300 kN capacity Shimadzu AGSX mechanical testing machine and TRAPEZIUM X testing software (Figure 3.10).

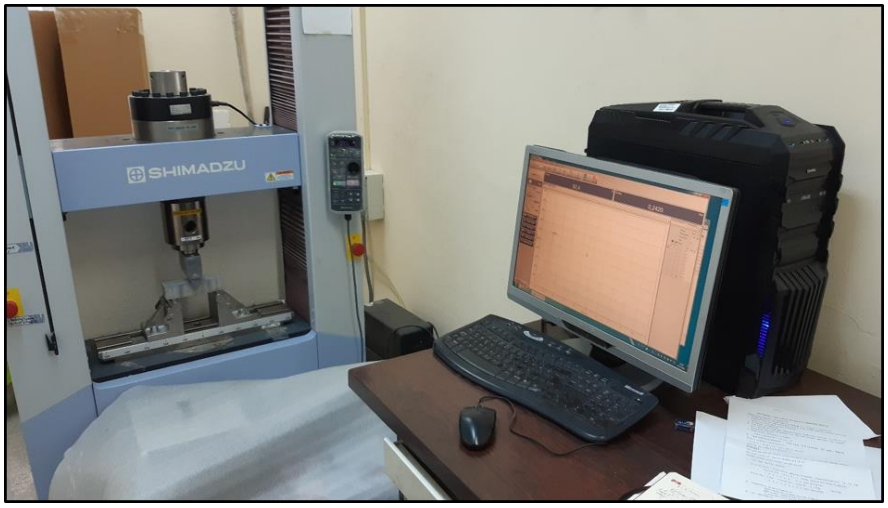


Figure 3.10 Shimadzu testing machine (Personal archive, 2020)

The technical specifications of the Shimadzu Signature AGS-300kNX apparatus used in the experiments are shown in Table 3.7. All results from measurements are reported as the average of at least three samples.

Table 3.7 The specifications of Shimadzu Apparatus (manufacturer data)

Capacity		300 kN
Loading Method		Direct, High Precision, constant-rate strain control using non-blacklash precision ball-screw drive
Sampling Speed		1000 Hz-max.
Speed Accuracy		±0.1%
Force Measurement Accuracy	**High Precision Type (1/500, ±0.5%)**	Within ±0.5% indicated test force (at 1/250 to 1/1 load cell rating), Conforms to EN 10002-2 Grade 0.5, ISO 7500-1 Class 0.5, BS 1610 Class 0.5, and ASTM E4, JIS B7721 Clas 0.5.
	Standard Precision Type (1/500, ±1%)	Within ±1% indicated test force (at 1/500 to 1/1 load cell rating), Conforms to EN 10002-2 Grade 1, ISO 7500-1 Class 1, BS 1610 Class 1, and ASTM E4, JIS B7721 Clas 1.
Crosshead	**Speed Range**	0.001 to 500 mm/min (stepless)
	Max. Return Speed	550 mm/min

3.2.4.1 Flexural Test

Flexural strength, defined as maximum stress, is a measure of a material's ability to withstand bending or bending stresses without breaking. According to ASTM C1609 (2012), the flexural strength of the 28-day-cured mortar blocks was calculated using the three-point loading method at a rate of 0.2 mm/min. The prism block has dimensions of 40 x 40 x 160 mm. The span length was 120 mm. All samples were initially loaded with 100 N at 0 stroke (Figure 3.11).

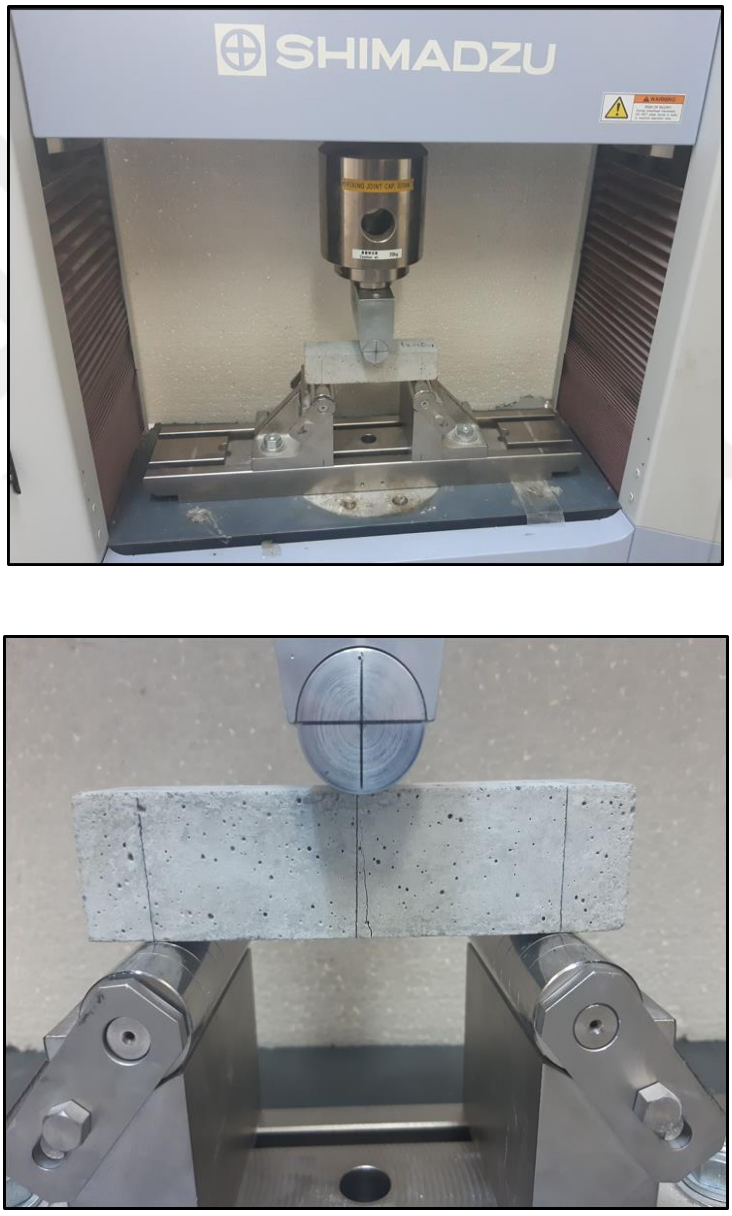


Figure 3.11 Three-point flexural test of mortar samples (Personal archive, 2020)

Flexural strength was calculated using Eq.3.3.

$$\sigma_f = 1.5\frac{PL}{bd^2} \tag{3.3}$$

Equation 3.3 has the following variables: (σ_f) the flexural strength in MPa, (P) the axial load at the point of failure in N, (L) is the span between two supports in mm, (b) specimen width in mm, *(d)* depth of the block at failure in mm. The area under the force-displacement curve was also used to compute the fracture energy.

3.2.4.2 Compression Test

The ability of the specimen to withstand fracture under axial force is known as compressive strength. According to ASTM C349 (2014), a compression test was carried out at a speed of 0.5 mm/min on both sides of the specimens that failed the flexure test. The blocks used in the experiment were cubic in shape with dimensions of 40 x 40 x 40 mm. Before the testing began, a force of 200 N was applied to all samples at 0 strokes. The tests were stopped when the force dropped to 50% of the maximum force reached (Figure 3.12).

Compressive strength was determined from equation 3.4.

$$\sigma_c = \frac{P}{b^2} \tag{3.4}$$

Where; σ_c the compressive strength in MPa, (P) the maximum stress in N and (b) the dimensions of the cube sample in mm. Compression fracture energies were calculated using the area under the load-displacement curves.

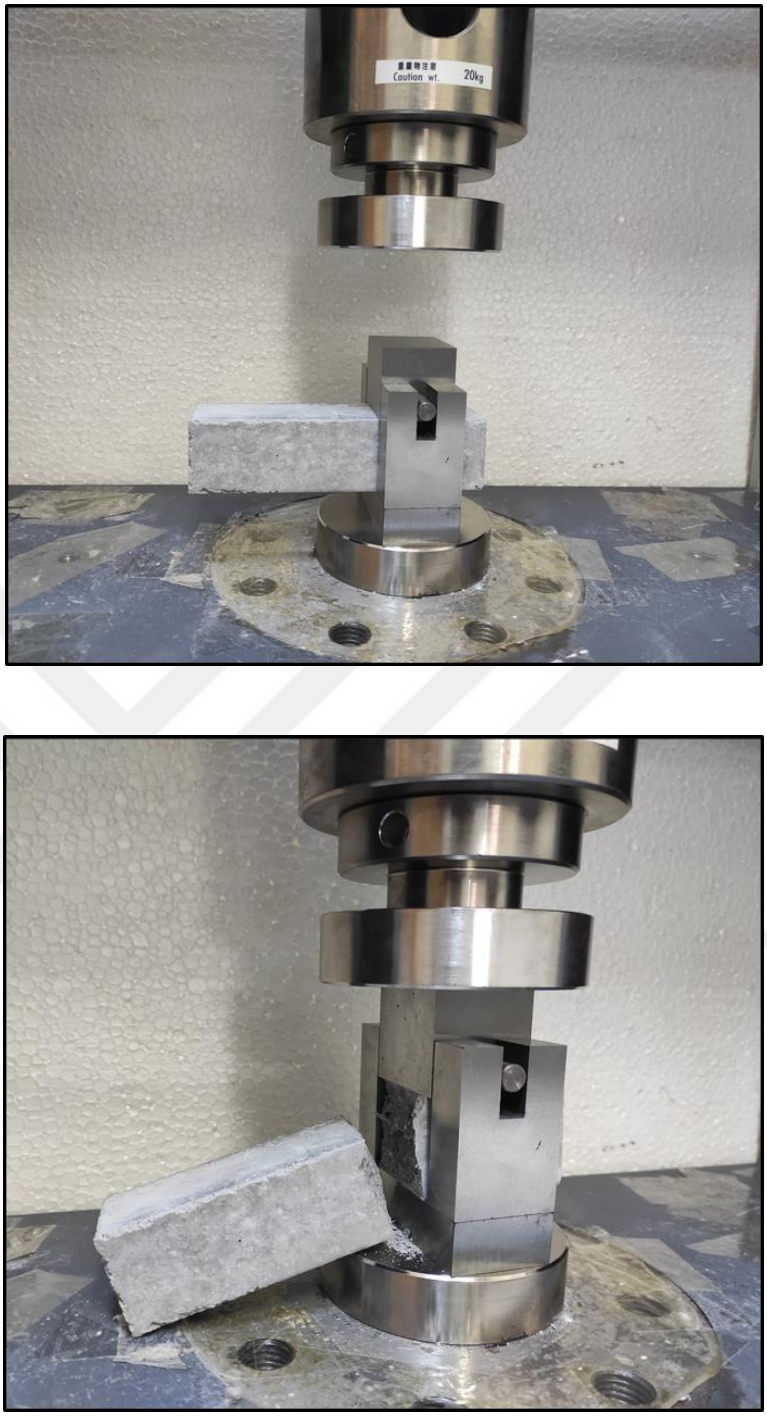


Figure 3.12 Compression test of mortar samples (Personal archive, 2020)

CHAPTER FOUR

RESULTS AND DISCUSSION

The findings of all experimental work and the impact of different factors on the mechanical characteristics and freshness of the mortar have been discussed in this part.

4.1 Biochar Properties

SEM images show that the biochar particles have a rough, irregular and heterogeneous surface with different particle size below 500 nm (Figure 4.1). The roughness and irregularity of the surface are important for the bonding between biochar and cement matrix (Figure 4.1a-b-c). The pores shown in Figure 4.1d are from apricot kernel shell biochar. It is formed by the release of volatile and organic matter during pyrolysis. The porosity caused by biochar can play an important role in water uptake and retention during internal curing (Gupta et al., 2018c).

Table 4.1 presents the elemental composition of the raw material and the nano biochar as determined by XPS. It can be observed that the apricot kernel has the highest carbon and no inorganic substances while the industrial and municipal sewage sludges have less carbon content and some metals such as iron, calcium, silicon, magnesium, aluminium. The apricot kernel biochar is more stable due to the carbon content of 87.67% with oxygen to carbon molar ratio (O/C) of 0.11. The O/C ratio determines the degree of the long-term stability of the biochar. According to common patterns, biochar with an O/C ratio of less than 0.20 has a strong tendency for stability. This trend indicates that biochar is an important factor that prevents the change of properties of the cement composite into which it is added (Spokas, 2010).

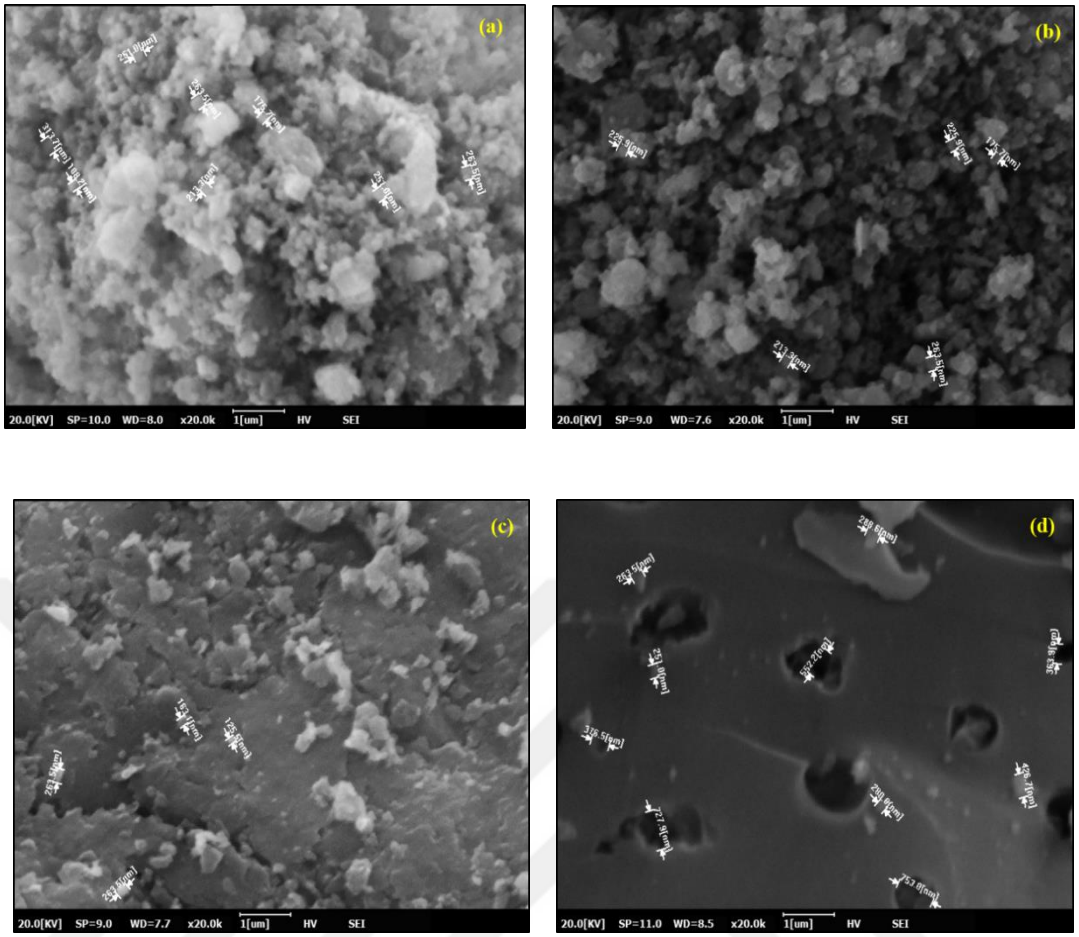


Figure 4.1 SEM images of (a) industrial chemical sludge nano biochar (b) industrial mixed sludge nano biochar (c) sewage sludge nano biochar (d) apricot kernel shell nano biochar

Table 4.1 Elemental composition of the samples (wt.%)

Name Code	C	O	Si	Al	Fe	Ca	Mg	Na	P	N	S	O/C
RC	34.96	31.63	5.43	-	18.13	1.31	-	-	3.52	2.46	2.58	0.68
BCC	27.87	28.19	6.79	-	14.27	3.85	1.72	1.65	-	1.86	4.48	0.76
RM	34.73	31.05	3.78	-	13.74	-	-	-		4.18	1.62	0.67
BCM	28.61	28.58	10.22	-	17.13	4.64	-	3.83		3.13	-	0.75
RSS	51.42	31.17	5.1	-	1.17	4.08	-	-	1.87	4.63	0.57	0.45
BCSS	44.46	27.29	8.6	3.68	-	6.29	1.22	1.13	2.81	4.52	-	0.46
RAK	70.47	28.38			-	0.34				0.81		0.30
BCAK	87.67	12.33	-	-	-	-	-	-		-	-	0.11

4.2 Flow of Mortar Mixtures

The flow of mortar related to workability is one of the most important fresh state properties. The flow of mortar mixtures is shown in Figure 4.2. In all volume percent, mortar with industrial mixed sludge nano biochar (BCM) had a lower flow with respect to CM while mortar with industrial chemical sludge nano biochar (BCC) had higher flow at low volume percent (0.04-0.06) and lower flow at higher volume percent (0.12-0.15) of nano biochar, as seen in Figure 4.2a. Mortar mixtures with sewage sludge nano biochar (BCSS) and apricot kernel shell nano biochar (BCAK) had varying results with respect to CM at different volume percent. The increase in flow can be due to the slippery surface of the nano biochar. However, the inclusion of 0.15% by volume of all-nano biochar leads to a decrease in flow characteristics. The decrease in flow observed in the mortar with a high concentration of nano biochar is thought to be caused by two factors. The mortar's fluidity decreases since nano biochar particles are porous, more water is retained. Additionally, the angular structure of the particles creates an impediment that slows the flow by preventing the mortar paste from moving freely.

Figure 4.2b demonstrates that adding a hybrid mix of apricot kernel shell and sewage sludge nano biochar improved the flow for all hybrid mixes when compared to the reference.

The raw industrial chemical (RC) and mixed sludge (RM) mixtures had a decrease of flow with respect to control mixture, which was due to the existence of metallic oxides such as iron oxide, silicon dioxide, which were hydrophilic in chemical and mixed industrial sludge. The hydrophilic compounds attracted water molecules, decreasing the free water and so the flow. Also, sludge particle agglomeration was effective in decreasing the flow, as seen in Figure 4.2c. The municipal raw sewage sludge (RSS) and raw apricot kernel shell (RAK) had a higher flow with respect to the control mixture, due to the higher carbon material content (presented in Table 4.1), which were hydrophobic, expelling water and increasing flow.

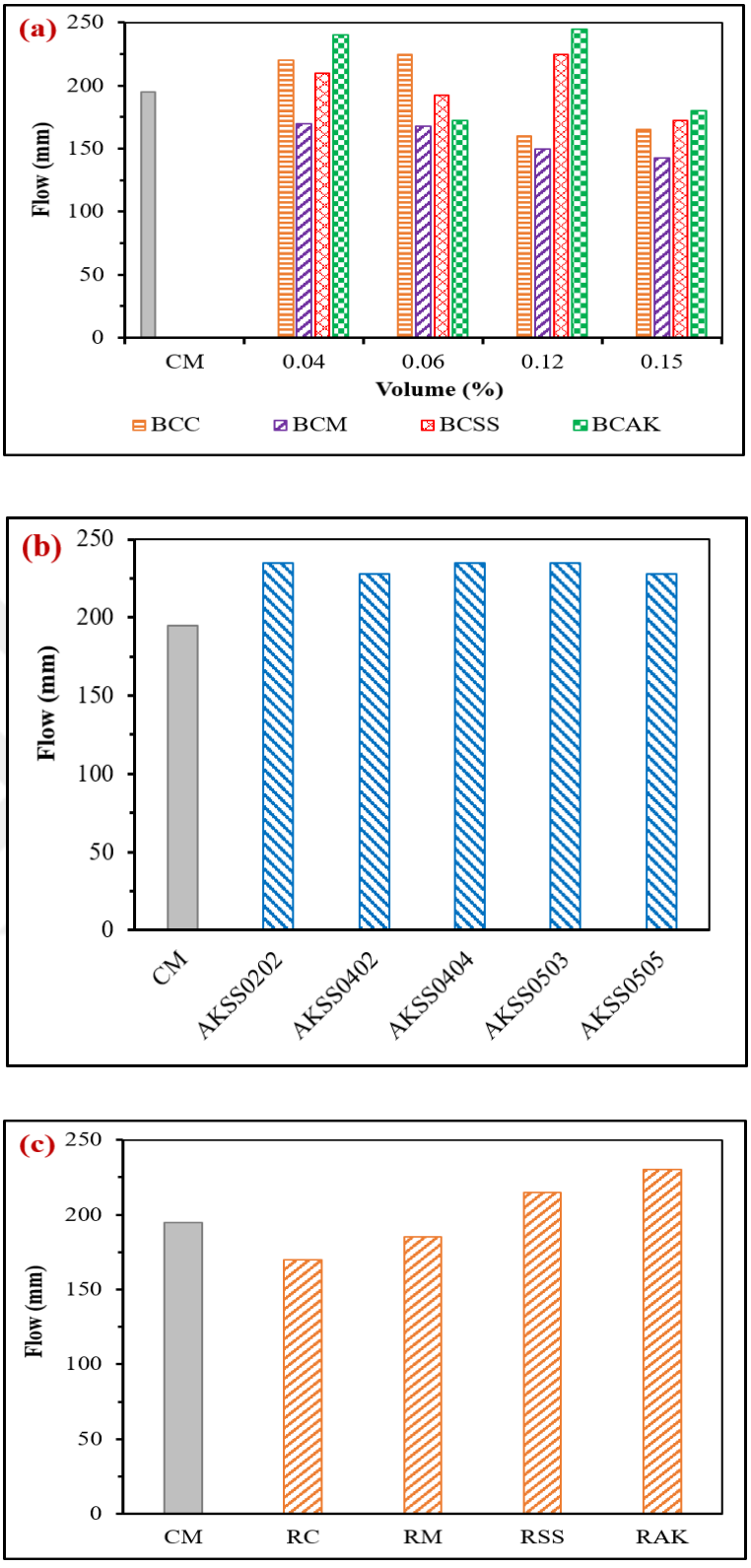


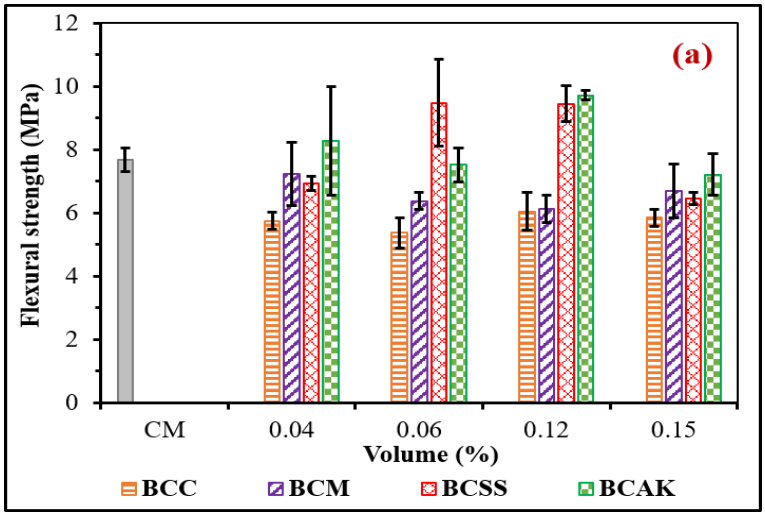
Figure 4.2 Flow of mortar mixtures with (a) different volume of nano biochar (b) different combinations of apricot kernel shell nano biochar and sewage sludge nano biochar (c) different raw material by 0.12 volume %

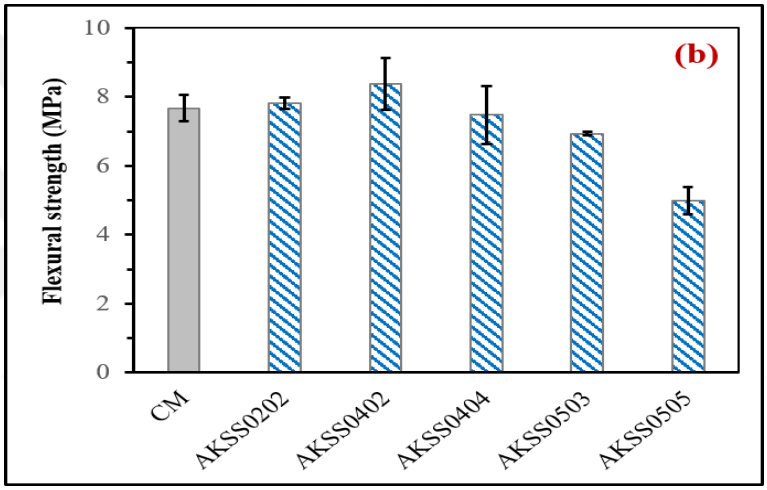
4.3 Flexural Strength and Energy of Mortar Blocks

The flexural strength of the mortar containing various nano biochar at various volume fractions is depicted in Figure 4.3a. The strength for bending of industrial chemical sludge nano biochar (BCC) and industrial mixed sludge nano biochar (BCM) mortar mixes decreased, while it increased for mortar mixtures containing of sewage sludge nano biochar (BCSS for 0.06 % and 0.12%) and apricot kernel shell nano biochar (BCAK for 0.12%). 0.06-0.12 vol.% sewage sludge nano biochar and 0.12 vol.% apricot kernel shell nano biochar provided the highest flexural strength: 9.47 MPa-9.45 MPa and 9.71 MPa, respectively, that were higher by 23.4%-23.1% and 27% compared to control mortar. These results can be explained by the carbon content in the biochar particles: 27.87%, 28.61%, 44.46%, 87.67% for BCC, BCM, BCSS, and BCAK, respectively (see Table 3.1). It can be said that a higher carbon content leads to increase flexural strength while a smaller carbon content results in particles with more faults and less mechanical resistance. The optimal nano biochar volume percentage was 0.12%, which resulted in an increase in strength for BCSS and BCAK.

Figure 4.3b illustrates the flexural strength of hybrid mortar incorporating varying amounts of apricot kernel shell nano biochar (BCAK) and sewage sludge nano biochar (BCSS). The maximum bending resistance value, 8.37 MPa, was obtained with the inclusion of AKSS0402. Compared with the reference mortar, the flexural strength increased by 1.9% for AKSS0202, and by 9.1% for AKSS0402. However, the addition of AKSS0404, AKSS0503, and AKSS0505 decreased the flexural strength of the mortar mixes. It can be said that apricot kernel shell nano biochar is more important than sewage sludge nano biochar for hybrid composite mortars due to its high carbon content. The flexural strength of mixtures with high-volume percent decreased due to agglomeration and formation of weak zones by nano biochar.

Figure 4.3c shows the flexural strength of mortar with different nano-sized raw materials. The inclusion of all raw materials resulted in a decrease in the flexural strength of the mortar when compared to the reference mortar mixture.





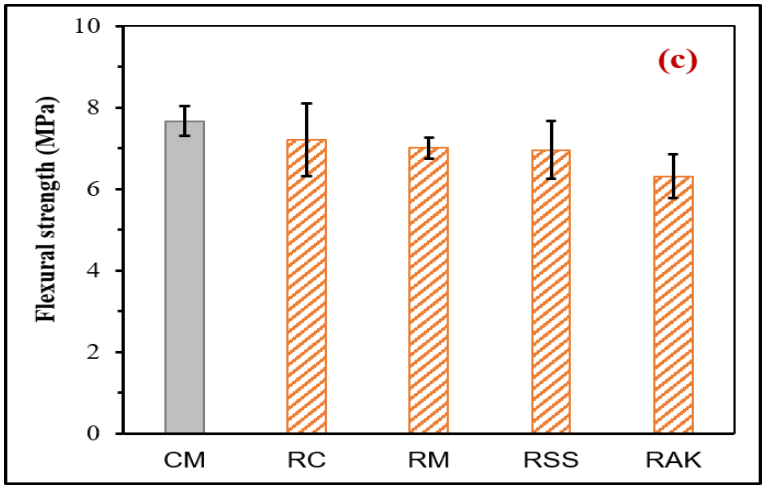


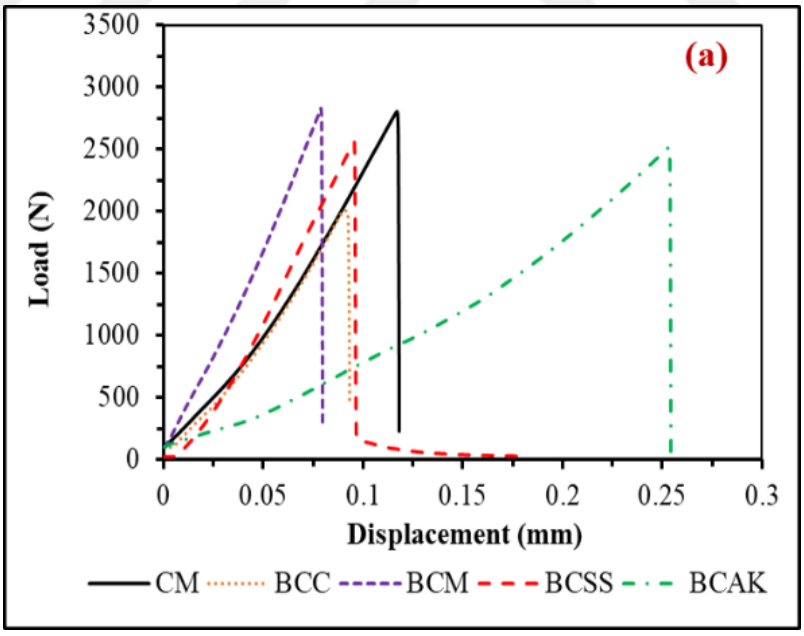
Figure 4.3 Flexural strength of mortar mixtures with (a) different volume of nano biochar (b) different combinations of apricot kernel shell nano biochar and sewage sludge nano biochar (c) different raw material by 0.12 volume %

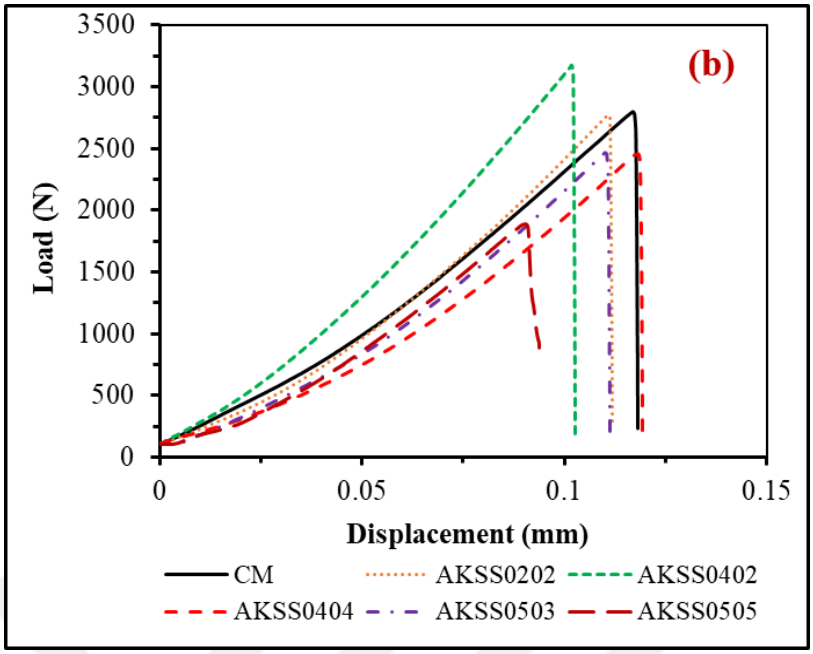
Typical load-midspan displacement curves from flexural tests for the mortar composites containing different nano biochar, AKSS-hybrid nano biochar, and raw material were presented in Figure 4.4.

The maximum displacement of a mixture with apricot kernel shell nano biochar was higher than that of the other mixtures (Figure 4.4a).

The mortar with AKSS0402 had a maximum peak load (Figure 4.4b). It can be said that apricot kernel shell nano biochar and AKSS0402-hybrid additives are effective in improving the crack resistance and altering the crack path in mortar, which increases the absorbed energy.

However, all the peak load values of mixtures with raw materials were small compared to the control mix (Figure 4.4c). The fracture energy of mortar block was determined by calculating the area under the load-displacement curve.





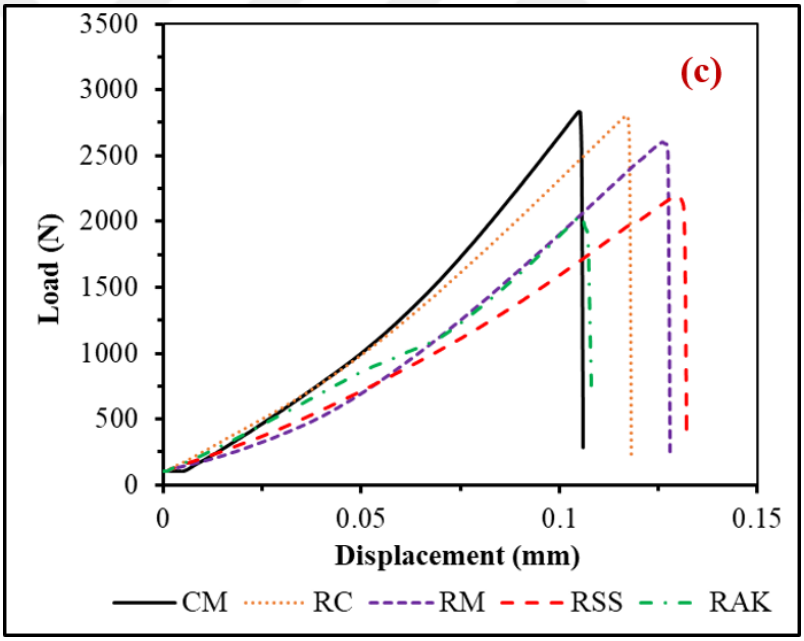
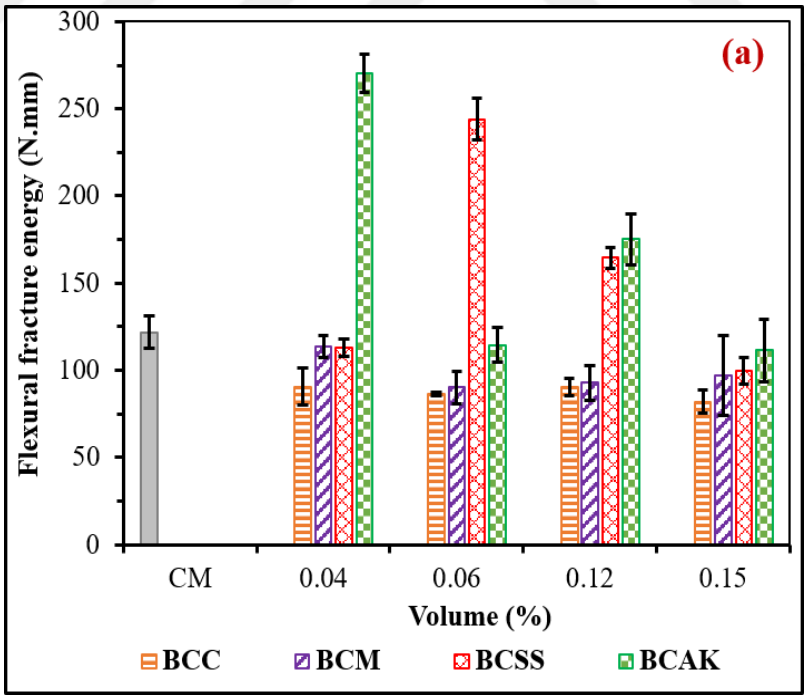


Figure 4.4 Load-midspan displacement curves for mortar composites at flexural tests with different (a) nano biochar at 0.04 vol.% (b) hybrid nano biochar (c) raw material at 0.12 vol.%

Figure 4.5a shows the flexural fracture energy of various mortars containing nano biochar. Fracture energy can be seen to be significantly greater for mortars containing 0.06 vol % sewage sludge nano biochar (BCSS) and 0.04 vol.% apricot kernel shell

nano biochar (BCAK). It was found that the usage of 0.06% BCSS and 0.04% BCAK by volume in the mortar increased the flexural fracture energy by 100% and 122%, respectively, while 0.12% BCSS and BACK by volume increased the energy by 35%, 44%, respectively, with respect to the control mortar. This indicates that the biochar in the mortar mix acted as a reinforcing agent. However, the mortar with BCC and BCM showed no improvement in energy performance. The dissimilarity in the behavior of load-displacement can be associated with the morphology of the particles in the mortar, including their roughness, angularity, and bonding. The angular shape of the biochar causes an enlargement in its surface area, which may improve its effectiveness in reinforcing the surrounding paste. Moreover, the addition of the nano biochar particles of irregular size created impenetrable barriers that resulted in a change in crack progression by increasing the tortuosity and pathway. The presence of a larger amount of materials during the fracture process promotes volumetric fracture rather than surface fracture, consequently increasing the fracture energy required for crack initiation and propagation.



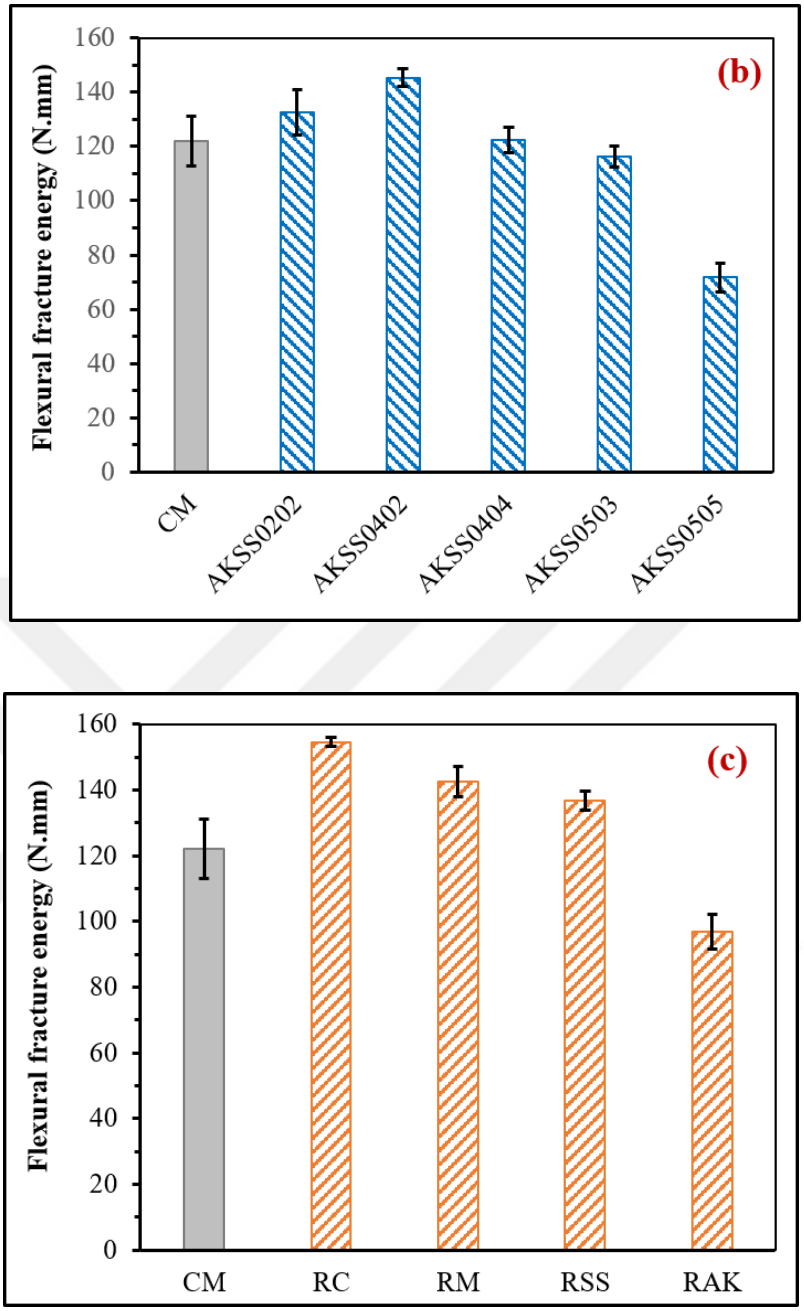


Figure 4.5 Flexural fracture energy of mortar mixtures with (a) different volume of nano biochar (b) different combinations of apricot kernel shell nano biochar and sewage sludge nano biochar (c) different raw material by 0.12 volume %

Figure 4.5b shows the flexural fracture energy of hybrid mortar mixes with the combination of apricot kernel shell and sewage sludge nano biochar. The addition of AKSS0402 provided the highest fracture energy value of 145.31 N.mm, which is 19% higher compared to the reference mortar. This is due to the fact that crack propagation

was deflected and more material was involved the failure process in the mortar. However, the other hybrid mixtures had no significant effect on the energy.

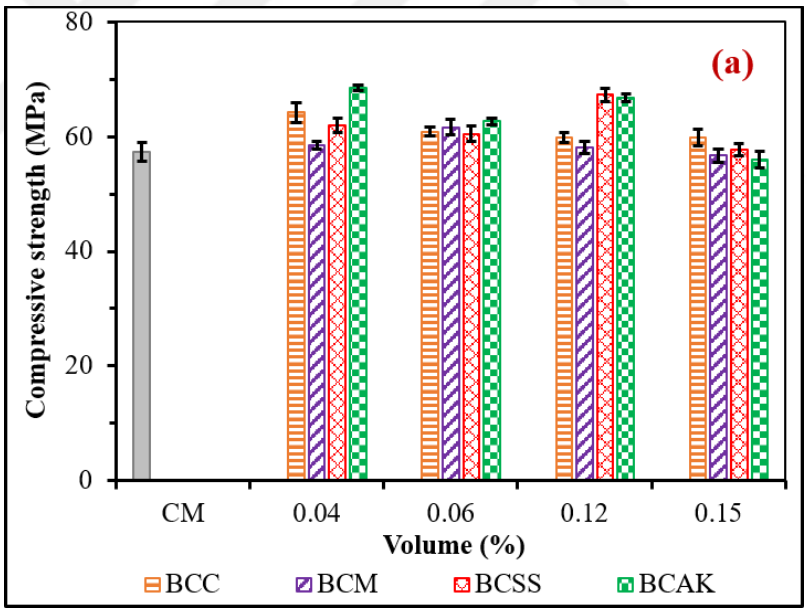
Figure 4.5c shows the fracture energy of mortar mixtures with different nano raw materials by 0.12 volume%. All nanoscale raw materials caused an increase in the fracture energy of mortar mixtures except apricot kernel shell (RAK). The admixture of industrial chemical sludge (RC), industrial mixed sludge (RM), and municipal sewage sludge (RSS) increased the fracture energy of mortar by 27%, 17%, 12% in comparison with the control mixture, respectively. The existence of nanoscale particles obstructed crack propagation, which resulted in an increase in energy.

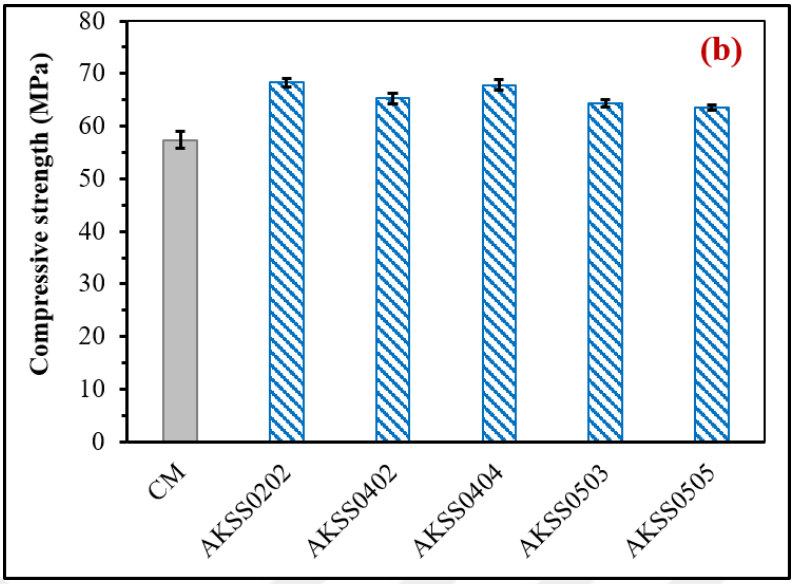
4.4 Compressive Strength and Energy of Mortar Blocks

The compressive strength of mortar containing different nano biochar is shown in Figure 4.6. There was an increasing trend in the compressive strength of all mortar combinations (Figure 4.6a). 0.04% by volume of BCAK, 0.12% by volume of BCSS, 0.04% by volume of BCC, and 0.06% by volume of BCM provided the highest compressive strength: 68.50 MPa, 67.28 MPa, 64.22 MPa, and 61.58 MPa successively, that were higher by 19%, 17%, 12%, and 7.3% compared to control mortar, respectively. One could conclude that the incorporation of biochar into the mixture up to a volume fraction of 0.12 results in a significant improvement in compressive strength.

Compressive strength can be increased through four different mechanisms. First, the addition of nano biochar to cementitious composites results in a nano-level pore filling effect, resulting in the refinement of the composite microstructure. It also creates nucleation sites for forming hydration products such as calcium silicate hydrate (CSH) and calcium silicate aluminium hydrate (CSAH) in the mortar matrix. Second, the incorporation of biochar can result in the absorption of a portion of the mixing water by porous biochar particles, thereby causing a decrease in the water-to-cement ratio of the mortar. This led to the densification of the soaked mortar by reducing the free water, leading to the formation of pores. In addition, the water retained in the biochar was subsequently released during the curing, leading to internal curing. As

SEM pictures of apricot kernel shell nano biochar display honeycomb-like pores because of a greater release of volatile gases and organic compounds during pyrolysis, this mechanism may be particularly effective in apricot kernel shell biochar composites. Third, the biochar particles have a rough, irregular and heterogeneous surface with smaller particle size. The roughness and irregularity of the surface is important for the bonding between biochar and cement matrix. Fourth, BCSS could promote the formation of extra CSH and CASH gel formed by the additional reaction due to the presence of silica, alumina, and calcium, thereby improving strength of the hydrated cement matrix. However, the addition of 0.15% nano biochar by volume exhibited a decreasing trend in compressive strength of mortar. The decrease could be due to the agglomeration of the nanostructured particles around the cement grains, which resulted in a delay in cement hydration. Furthermore, the defects that occur during the dispersion of nanoparticles contribute to the formation of weak zones.





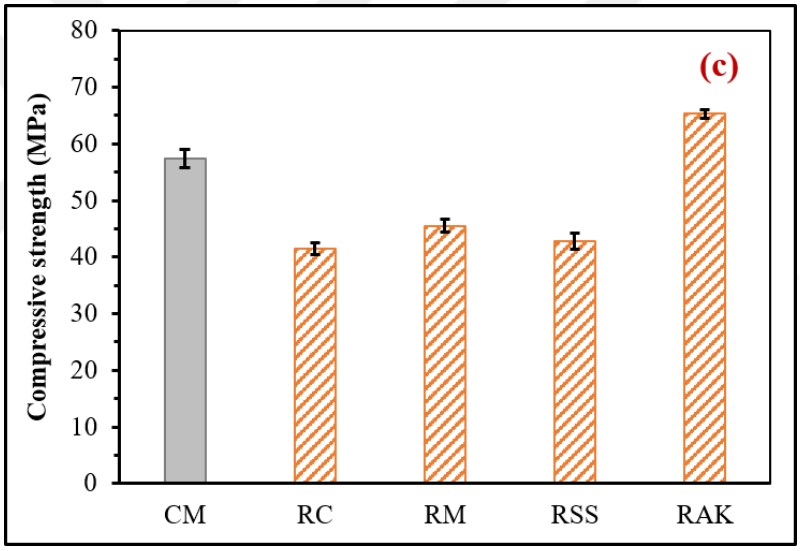


Figure 4.6 Compressive strength of mortar mixtures with (a) different volume of nano biochar (b) different combinations of apricot kernel shell nano biochar and sewage sludge nano biochar (c) different raw material by 0.12 volume %

The compressive strength of hybrid mortars with various quantities of apricot kernel shell and sewage sludge nano biochar was investigated (Figure 4.6b). The results showed that all hybrid mixtures had greater compressive strengths with respect to the control mixture, indicating that the addition of these nano biochar improved the mortar's mechanical qualities. AKSS0202, AKSS0402, AKSS0404, AKSS0503, and AKSS0505 exhibited a compressive strength of: 68.34 MPa, 65.25 MPa, 67.86 MPa,

64.31 MPa, 63.50 MPa, respectively, which were 19%, 14%, 18%, 12%, and 11% higher compared with the reference mix. The increase in compressive strength observed upon adding nano biochar can be attributed to the effect of pore-filling and internal hardening. The smaller biochar particles are thought to provide nucleation sites that help produce hydration products in the mortar matrix and refine the microstructure of cementitious composites. The porous biochar particles in the mixture also retained a certain amount of the mixing water, which was subsequently released into the mortar paste during the curing process. However, an excessive increase in the volume ratio of the nano biochar led to a reduction in the compression strength caused by the agglomeration.

The compressive strength of mortar containing various nanoscale raw materials at 0.12% by volume was shown in Figure 4.6c. Only the addition of apricot kernel shells with high carbon content increased the compressive strength of the mortar by 14% compared to the reference mortar. Sewage sludge, chemical, and mixed sludges contain impurities such as metals and compounds (see Table 4.1). Therefore, due to poor dispersion, agglomeration zones are formed in the mortar, which reduces the compressive strength.

Load-displacement curves obtained from the compression test for the mortar composites containing different nano biochar, AKSS-hybrid nano biochar and raw material were presented in Figure 4.7.

It can be observed that the maximum load is higher for mixtures with all nano biochar, hybrid combination of apricot kernel shell nano biochar and sewage sludge nano biochar, and only the raw apricot kernel shells with respect to reference mortar.

The mixture with apricot kernel shell had the highest load in all nano biochar as seen in Figure 4.7a; while AKSS0202 and AKSS0404 had the highest load among the hybrid mixtures, as presented in Figure 4.7b. In addition, raw apricot kernel shell yields the highest load amongst the raw material mixtures, as seen in Figure 4.7c.

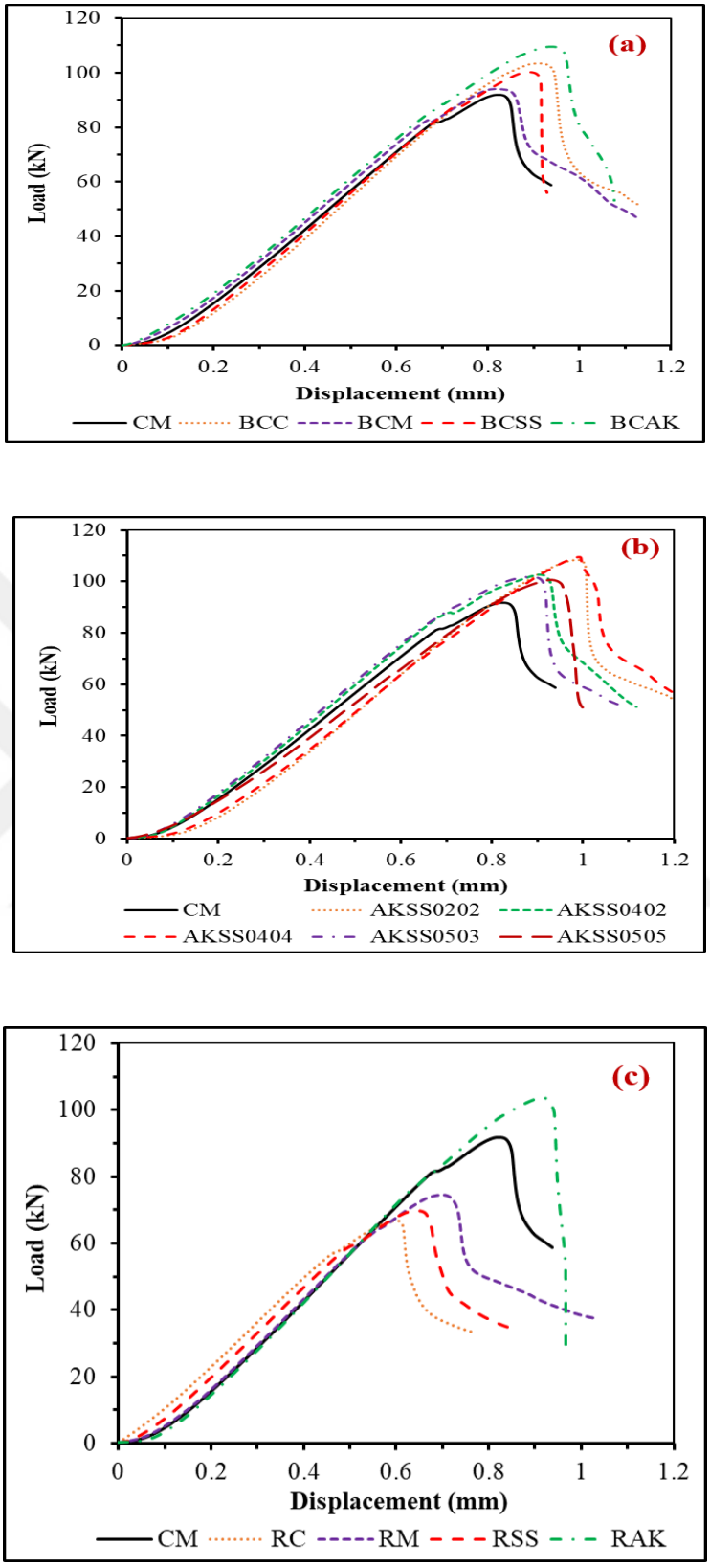
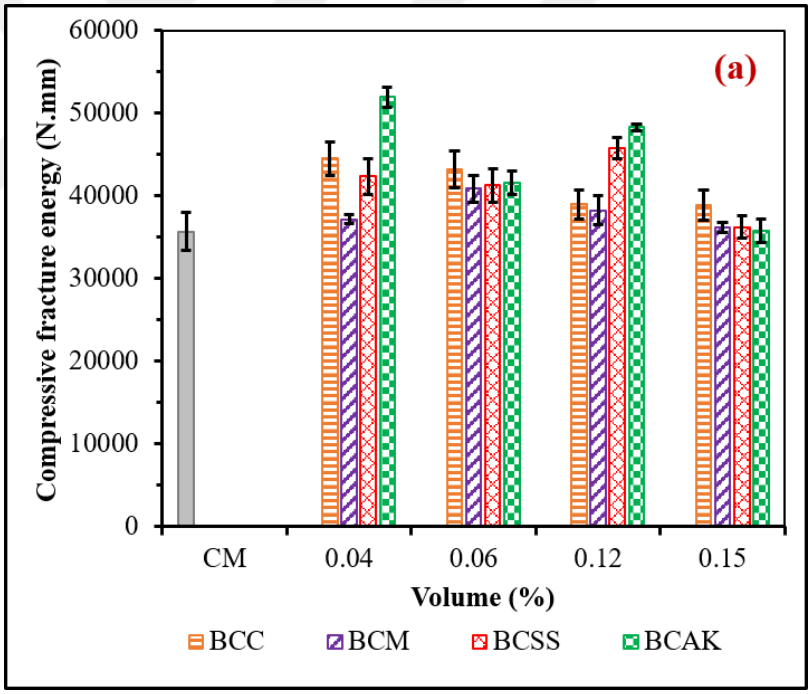
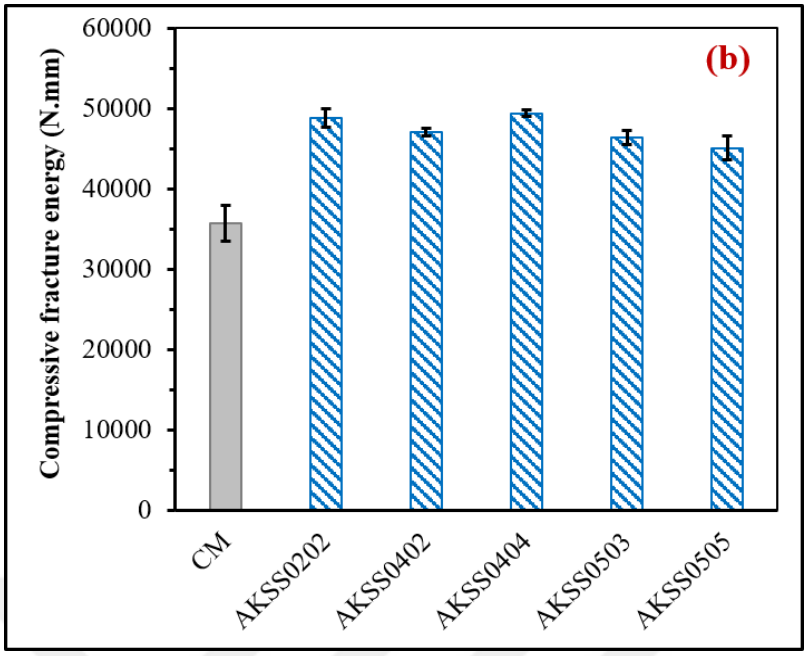


Figure 4.7 Load-displacement profile for mortar composites with different (a) nano biochar at 0.04 vol.% (b) hybrid nano biochar (c) raw material at 0.12 vol.% from compression tests

Similar trends in compressive strength can be observed in the plots of compression fracture energy depicted in Figure 4.8. The addition of 0.04 vol.% of apricot kernel shell nano biochar (BCAK) resulted in the highest increase in fracture energy, with a 45% improvement. Additionally, incorporating 0.12 vol.% of sewage sludge nano biochar (BCSS) and BCAK increased the energy of the mortar by 28% and 35% respectively, compared to the control mortar (Figure 4.8a). It can be suggested that the influence of the micro-filler of inert carbon particles on the paste is more significant than the impact of the pozzolanic reaction. At low and medium volume percentages, the nano biochar particles deflected the crack path and effectively filled the voids within the mortar mix, providing strong inclusions. However, at 0.15vol.%, the compression fracture energy showed minimal variation compared to the reference mortar due to the agglomeration of the nano biochar particles.





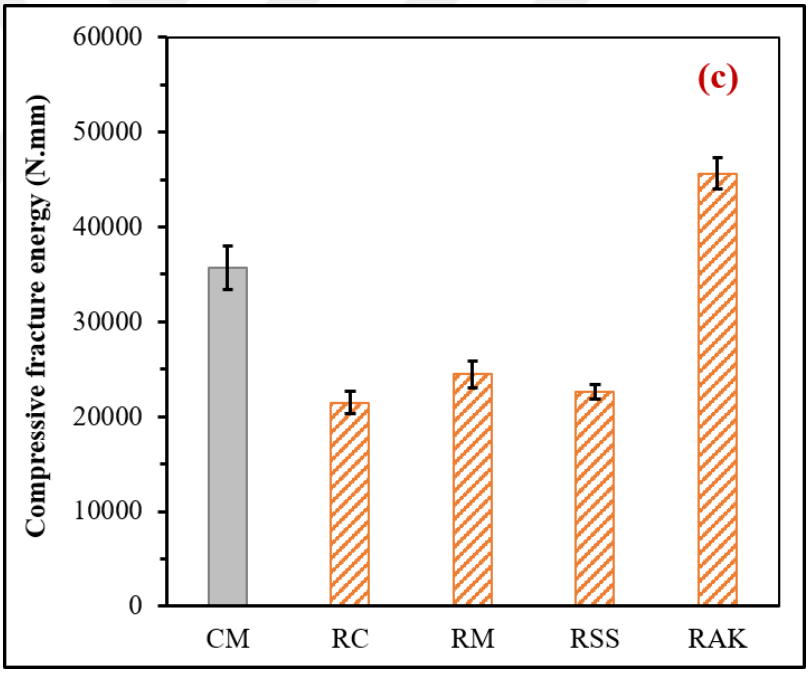


Figure 4.8 Compression fracture energy of mortar mixtures with (a) different volume of nano biochar (b) different combinations of apricot kernel shell nano biochar and sewage sludge nano biochar (c) different raw material by 0.12 volume %

Figure 4.8b shows the fracture energy of hybrid mortar mixes with the combination of apricot kernel shells and sewage sludge nano biochar. The compressive fracture energy also enhanced by the addition of mixed biochar. The addition of AKSS0202

and AKSS0404 caused the highest increase in the compression fracture energy of the mortar mixtures of 37%, 38% respectively, compared to the reference. The reason for this can be that, the nano biochar particles dissipate cracks and act as strong inclusions filling the voids at low volume percent.

Figure 4.8c shows the compressive fracture energy of mortar mixtures with different raw materials by 0.12 vol.%. The addition of apricot kernel shells increased the compression fracture energy of the mortar by 28% compared to reference mortar mix, while the addition of sewage sludge, industrial chemical, and industrial mixed sludge resulted in a decrease in compressive fracture energy. This can be defined as a result of explained due to the higher carbon content and porous structure of apricot kernel shell. The higher carbon content provides a better inclusion, which increased the energy.

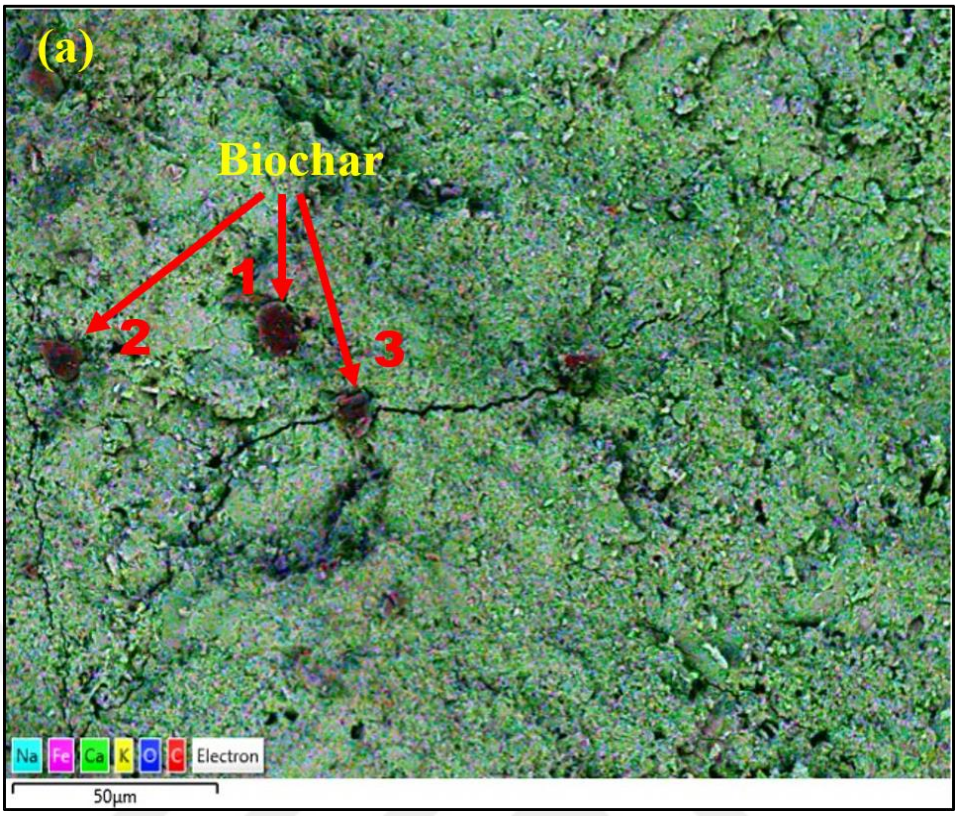
4.5 Micro Structural Analysis by SEM-EDS of Mortar

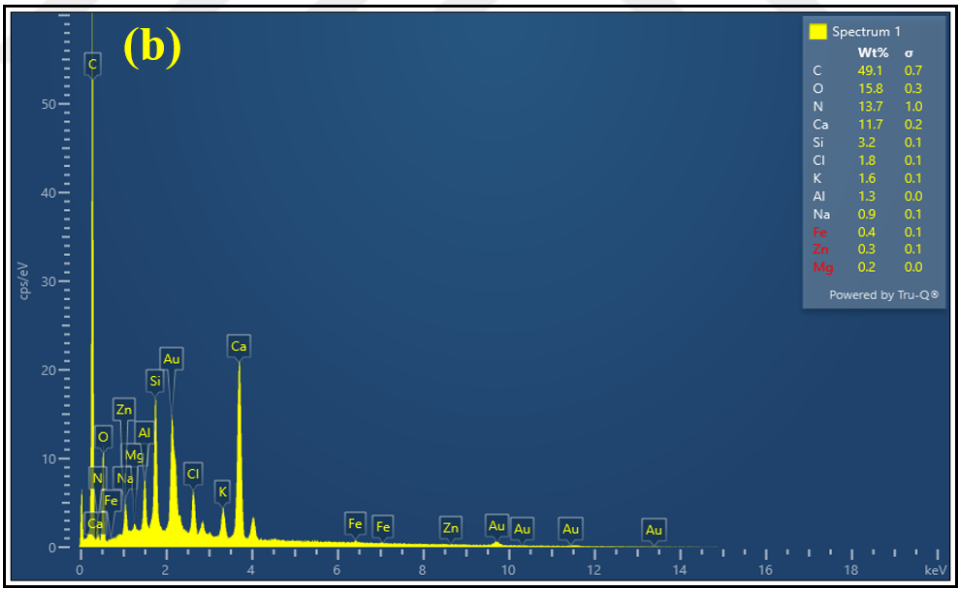
SEM-EDS images of the typical fracture surfaces of cementitious composite blocks incorporating nano biochar particles are depicted in the following Figure 4.9-10-11.

Nano biochar particles can affect the cement matrix in four ways:

i) SEM-EDS layered images in Figure 4.9a-b-c-d show that point 1, point 2, and point 3 have 49.1%, 47.7%, and 41.7% carbon (C), respectively. Therefore, these points are nano biochar particles. The pore-filling effect brought forth by the finer biochar particles refined the pore structure of cementitious composites, thus the smaller pores would increase the strength.

ii) The nano biochar particles affected the growing crack path (Figure 4.10). In the reference mortar, the sudden failure occurs after the crack develops while in the mortar with biochar, the biochar particles act as obstacles and divert crack propagation, causing more material to be involved in the failure process. This situation improves the flexibility and energy absorbing capacity of the self-strengthening cementitious composites.


(a)
Biochar
1
2
3
Na
Fe
Ca
K
O
C
Electron
50µm


(b)
Spectrum 1
Wt% σ
C 49.1 0.7
O 15.8 0.3
N 13.7 1.0
Ca 11.7 0.2
Si 3.2 0.1
Cl 1.8 0.1
K 1.6 0.1
Al 1.3 0.0
Na 0.9 0.1
Fe 0.4 0.1
Zn 0.3 0.1
Mg 0.2 0.0
Powered by Tru-Q®
cps/eV
keV

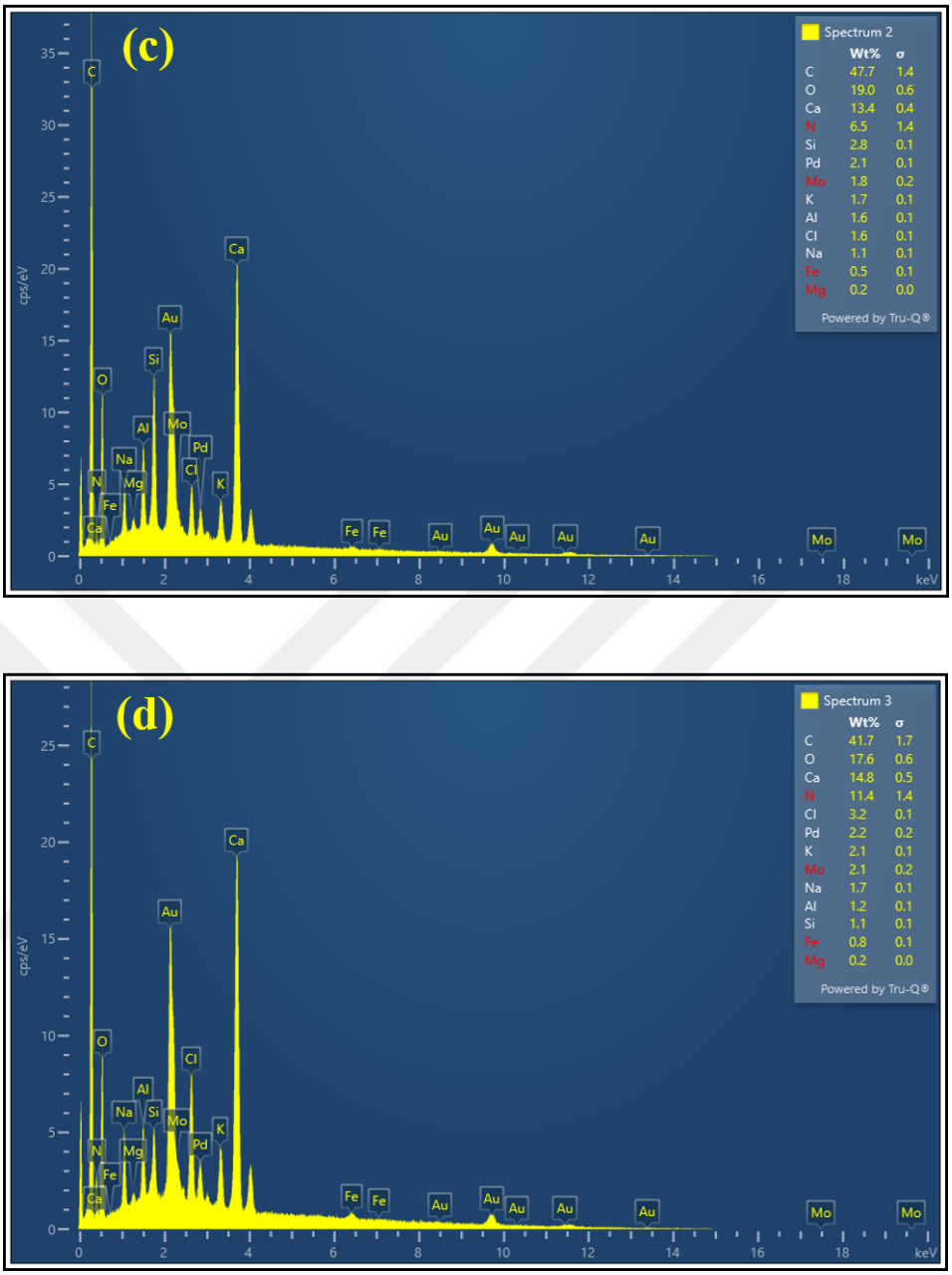


Figure 4.9 SEM-EDS micrograph of mortar with apricot kernel shell biochar

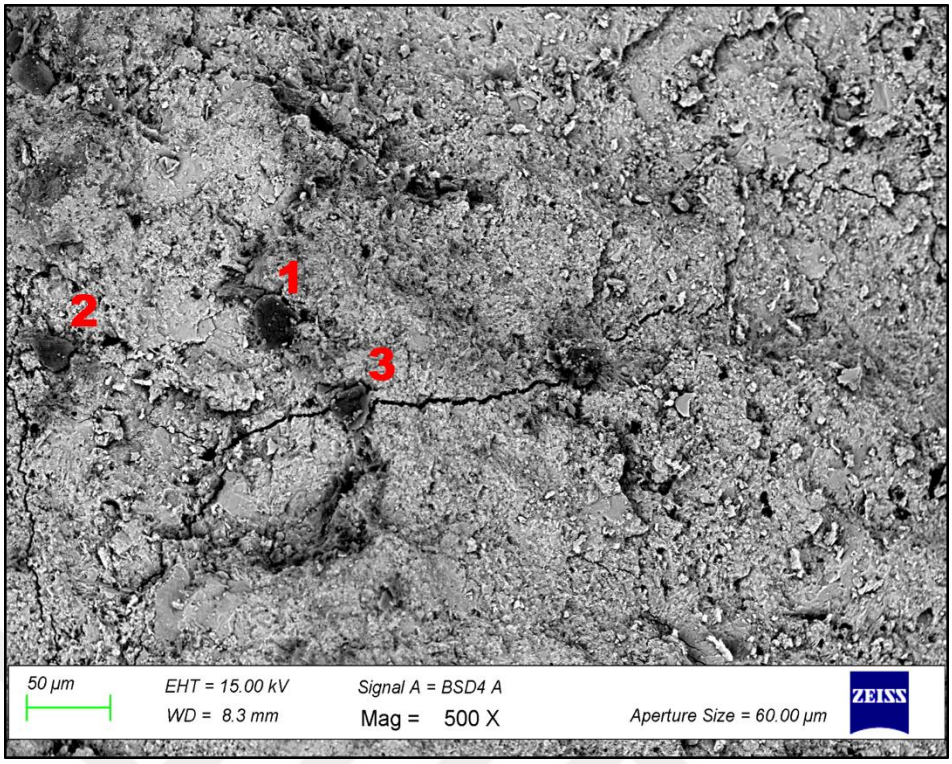
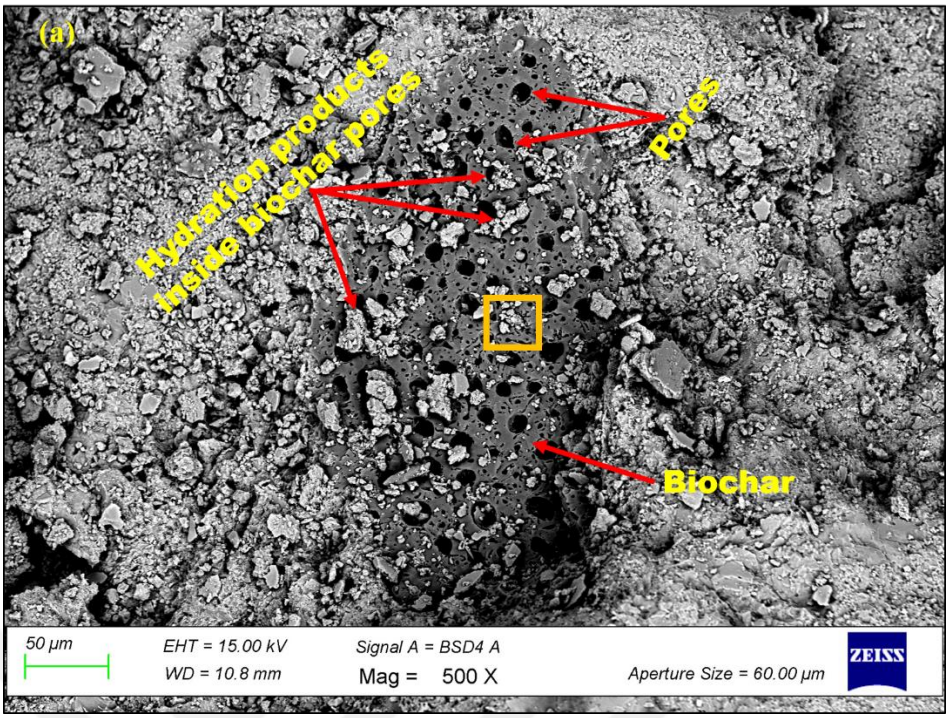


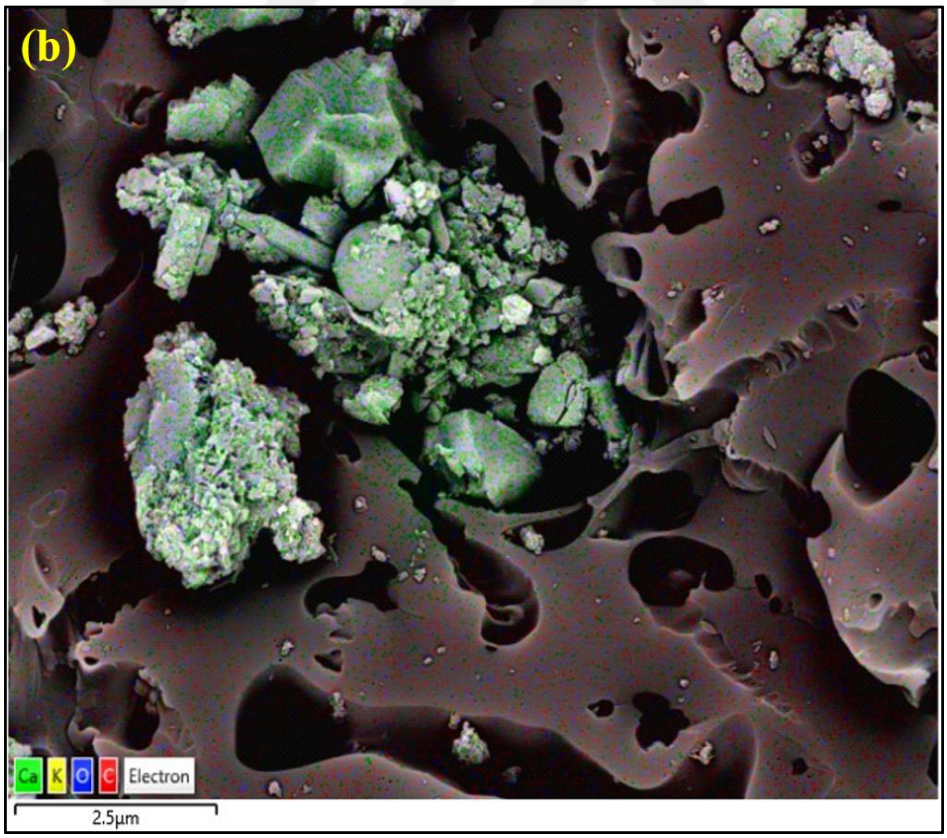
Figure 4.10 Divert crack propagation in mortar matrix

iii) Figure 4.11a shows that the nano biochar possesses a porous structure due to the pyrolysis process. These pores are responsible for high water absorption, which is later released to generate an internal curing effect caused to produce extra hydration products.

iv) Zooming in on the box in Figure 4.11a; the increased surface area of the nano biochar and the pores in biochar allowed for more nucleation areas where hydration products, such as C-S-H, could form, which plays a crucial role in determining the mechanical and physical characteristics of mortar pastes (Figure 11b-c).

However, incorporating 0.15vol.% of all nano biochars resulted in a decrease in flexural strength compared to the control mortar. The loss of flexural strength could be related to the agglomeration of biochar particles. The excessive dosage of nano biochar tends to trap air, leading to the formation of pores and acting as a weak site for crack propagation.


(a)
Hydration products inside biochar pores
Pores
Biochar
50 µm
EHT = 15.00 kV
WD = 10.8 mm
Signal A = BSD4 A
Mag = 500 X
Aperture Size = 60.00 µm
ZEISS


(b)
Ca
K
O
C
Electron
2.5µm

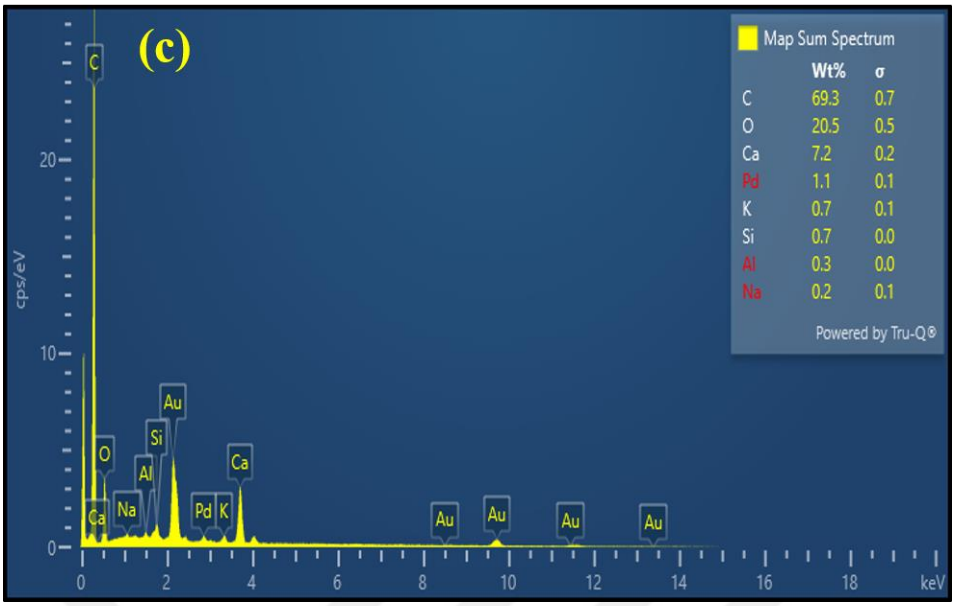


Figure 4.11 (a) SEM image of biochar (b) SEM zoom to the square window (c) SEM-EDS micrograph of deposition of hydration products inside the pores of biochar in mortar

CHAPTER FIVE

CONCLUSIONS AND FUTURE PLANS

5.1 Conclusions

The objective of this study was to examine the potential enhancement of mechanical properties in cement mortar through the incorporation of nano biochar as an additive. Biochar obtained through the pyrolysis process at 500°C from various sources such as industrial chemical and mixed sludge, municipal sewage sludge, and apricot kernel shells was finely ground to the nanoscale. Subsequently, different volume percentages of the nano-sized biochar were added to the mortar mixture. From the test results, the following conclusions were drawn:

* Flow of mortar was significantly influenced by nano biochar from industrial chemicals and mixed sludge due to low carbon content and higher amount of ash, while nano biochar from municipal sewage sludge and apricot kernel shell increased the flow because of high carbon content and slippery surface except by 0.06 vol.%. However, when a higher volume dosage of biochar at 0.15% was used, it caused a reduction in the flowability of the mortar. This decrease in flowability can be attributed to the biochar's high-water absorption capacity, the presence of particle shapes that hindered movement, and the agglomeration of biochar particles. The flow increased for all hybrid mixes (municipal sewage sludge and apricot kernel shell) compared to the control mixture. The industrial raw sludge (chemical and mixed) reduced the flow due to the hydrophilic nature that has more metal oxide compounds.

* The mortar containing 0.06% municipal sewage sludge nano biochar and 0.12% by volume apricot kernel shell nano biochar increased the flexural strength by 23%, 27%, while 0.06% municipal sewage sludge nano biochar and 0.04% apricot kernel shell nano biochar increased the flexure fracture energy by 100%, 122%, compared to the reference mortar. Flexural strength improved by 9.1%, and fracture energy increased by 19%, after the mortar mixture contained a hybrid of 0.04% apricot kernel

shell nano biochar and 0.02% sewage sludge nano biochar. The raw apricot kernel shell increased the fracture energy of the mortar by between 12%-26%.

* The mortar containing 0.12% volume of nano biochar derived from municipal sewage sludge and 0.04% volume of nano biochar derived from apricot kernel shell increased the compressive strength by 17% and 19%, also increased the compressive fracture energy by 28% and 45%, respectively, in comparison to the control mortar mix. The mortar mixture with a hybrid combination of 0.02% apricot kernel shell nano biochar and 0.02% sewage sludge nano biochar showed a 19% increase in compressive strength and a 37% increase in compressive fracture energy. The mortar with only raw apricot kernel shell increased compressive strength by 14% and the fracture energy by 28%.

* Depending on the type of waste biomass and production circumstances, the ideal dose range is considered to be between 0.04-0.12% by volume of municipal sewage sludge and apricot kernel shell biochar.

According to experimental results, the flexural strength, compressive strength, and fracture energy of cement-biochar composite mortar are significantly impacted by the nano biochar particles. The nanoparticles can act as a filler additive, reducing porosity and thereby densifying the mortar matrix and the aggregate/paste interface zone. Some nanoparticles, a high surface area to volume ratio and high reactivity, not only operate as obstacles to redirect the cracks increasing the volume of the fracture process, but also serve as nucleation sites for cement phases and enhance cement hydration. However, nanoparticle agglomeration at high doses of biochar can increase entrapped air voids and decrease the strength of mortar composites. Therefore, the effective dispersion technique of employing an ultrasonic bath to disperse nanoparticles in deionized water was used to reduce the agglomeration issue. The inclusion of biochar into mortar not only improves its mechanical properties, but also offers an opportunity for recycling waste biomass. Biochar used in mortar also helps to reduce greenhouse gas emissions by sequestering carbon.

5.2 Future Plan

This study examined how incorporating biochar into mortar affects its mechanical properties, but future research should focus on the properties and other benefits of biochar. These include a) investigating the possible environmental advantages of replacing cement with biochar to sequester carbon, b) studying the impact of combining biochar with silica fume, c) evaluating the efficacy of biochar produced at various temperatures, including 400, 600, and 700°C at other techniques, and d) investigating the use of biochar in the development of smart and multifunctional cement composites for self-sensing applications.

REFERENCES

Abhishek, K., Shrivastava, A., Vimal, V., Gupta, A. K., Bhujbal, S. K., Biswas, J. K., Singh, L., Ghosh, P., Pandey, A., Sharma, P., & Kumar, M. (2022). Biochar application for greenhouse gas mitigation, contaminants immobilization and soil fertility enhancement: A state-of-the-art review. *Science of the Total Environment*, 853, 158562. https://doi.org/10.1016/j.scitotenv.2022.158562

Ahmad, M., Soo Lee, S., Yang, J. E., Ro, H. M., Han Lee, Y., & Sik Ok, Y. (2012). Effects of soil dilution and amendments (mussel shell, cow bone, and biochar) on Pb availability and phytotoxicity in military shooting range soil. Ecotoxicology and Environmental Safety, 79, 225–231. https://doi.org/10.1016/j.ecoenv.2012.01.003

Ahmad, S., Khushnood, R. A., Jagdale, P., Tulliani, J. M., & Ferro, G. A. (2015). High performance self-consolidating cementitious composites by using micro carbonized bamboo particles. *Materials and Design*, 76, 223–229. https://doi.org/10.1016/j.matdes.2015.03.048

Akhtar, A., & Sarmah, A. K. (2018). Novel biochar-concrete composites: Manufacturing, characterization and evaluation of the mechanical properties. *Science of the Total Environment*, 616–617, 408–416. https://doi.org/10.1016/j.scitotenv.2017.10.319

Al-Hagri, M. G., & Döndüren, M. S. (2022). Effect and optimization of incorporation of nano-SiO2 into cement-based materials – a review. *Challenge Journal of Concrete Research Letters*, 13(1), 36. https://doi.org/10.20528/cjcrl.2022.01.004

Al-Rifaie, W. N., & Ahmed, W. K. (2016). Effect of Nanomaterials in Cement Mortar Characteristics. *Journal of Engineering Science and Technology*, 11(9), 1321-1332.

Amalina, F., Razak, A. S. A., Krishnan, S., Sulaiman, H., Zularisam, A. W., & Nasrullah, M. (2022). Biochar production techniques utilizing biomass waste-

derived materials and environmental applications – A review. *Journal of Hazardous Materials Advances*, 7, 100134. https://doi.org/10.1016/j.hazadv.2022.100134

Andrew, R. M. (2019). Global CO_2 emissions from cement production 1928 – 2018. *Earth System Science Data*, 11(4), 1675–1710. https://doi.org/10.5194/essd-11-1675-2019

Antal, M. J., Mochidzuki, K., & Paredes, L. S. (2003). Flash carbonization of biomass. *Industrial and Engineering Chemistry Research*, 42(16), 3690–3699. https://doi.org/10.1021/ie0301839

Antero, R. V. P., Alves, A. C. F., de Oliveira, S. B., Ojala, S. A., & Brum, S. S. (2020). Challenges and alternatives for the adequacy of hydrothermal carbonization of lignocellulosic biomass in cleaner production systems: A review. *Journal of Cleaner Production*, 252, 119899. https://doi.org/10.1016/j.jclepro.2019.119899

Asensio, V., Vega, F. A., Andrade, M. L., & Covelo, E. F. (2013). Tree vegetation and waste amendments to improve the physical condition of copper mine soils. *Chemosphere*, 90(2), 603–610. https://doi.org/10.1016/j.chemosphere.2012.08.050

Ayiania, M., Carbajal-Gamarra, F. M., Garcia-Perez, T., Frear, C., Suliman, W., & Garcia-Perez, M. (2019). Production and characterization of H2S and PO43− carbonaceous adsorbents from anaerobic digested fibers. *Biomass and Bioenergy*, 120, 339–349. https://doi.org/10.1016/j.biombioe.2018.11.028

Barskov, S., Zappi, M., Buchireddy, P., Dufreche, S., Guillory, J., Gang, D., Hernandez, R., Bajpai, R., Baudier, J., Cooper, R., & Sharp, R. (2019). Torrefaction of biomass: A review of production methods for biocoal from cultured and waste lignocellulosic feedstocks. *Renewable Energy*, 142, 624–642. https://doi.org/10.1016/j.renene.2019.04.068

Batidzirai, B., Mignot, A. P. R., Schakel, W. B., Junginger, H. M., & Faaij, A. P. C. (2013). Biomass torrefaction technology: Techno-economic status and future prospects. *Energy*, 62, 196–214. https://doi.org/10.1016/j.energy.2013.09.035

Beckinghausen, A., Reynders, J., Merckel, R., Wu, Y. W., Marais, H., & Schwede, S. (2020). Post-pyrolysis treatments of biochars from sewage sludge and A. mearnsii for ammonia (NH4-n) recovery. *Applied Energy*, 271(May), 115212. https://doi.org/10.1016/j.apenergy.2020.115212

Behazin, E., Ogunsona, E., Rodriguez-Uribe, A., Mohanty, A. K., Misra, M., & Anyia, A. O. (2016). Mechanical, chemical, and physical properties of wood and perennial grass biochars for possible composite application. *BioResources*, 11(1), 1334–1348. https://doi.org/10.15376/biores.11.1.1334-1348

Benedetti, V., Patuzzi, F., & Baratieri, M. (2018). Characterization of char from biomass gasification and its similarities with activated carbon in adsorption applications. *Applied Energy*, 227(August 2017), 92–99. https://doi.org/10.1016/j.apenergy.2017.08.076

Brown, R. A., Kercher, A. K., Nguyen, T. H., Nagle, D. C., & Ball, W. P. (2006). Production and characterization of synthetic wood chars for use as surrogates for natural sorbents. *Organic Geochemistry*, 37(3), 321–333. https://doi.org/10.1016/j.orggeochem.2005.10.008

Bruun, E. W., Ambus, P., Egsgaard, H., & Hauggaard-Nielsen, H. (2012). Effects of slow and fast pyrolysis biochar on soil C and N turnover dynamics. *Soil Biology and Biochemistry*, 46, 73–79. https://doi.org/10.1016/j.soilbio.2011.11.019

Cao, M., Zhang, C., & Wei, J. (2013). Microscopic reinforcement for cement based composite materials. *Construction and Building Materials*, 40, 14–25. https://doi.org/10.1016/j.conbuildmat.2012.10.012

Carvalho, J., Nascimento, L., Soares, M., Valério, N., Ribeiro, A., Faria, L., Silva, A., Pacheco, N., Araújo, J., & Vilarinho, C. (2022). Life Cycle Assessment (LCA) of Biochar Production from a Circular Economy Perspective. *Processes*, 10(12), 2684. https://doi.org/10.3390/pr10122684

Cha, J. S., Park, S. H., Jung, S. C., Ryu, C., Jeon, J. K., Shin, M. C., & Park, Y. K. (2016). Production and utilization of biochar: A review. *Journal of Industrial and Engineering Chemistry*, 40, 1–15. https://doi.org/10.1016/j.jiec.2016.06.002

Cosentino, I., Restuccia, L., Ferro, G. A., & Tulliani, J. M. (2018). Influence of pyrolysis parameters on the efficiency of the biochar as nanoparticles into cement-based composites. *Procedia Structural Integrity*, 13, 2132–2136. https://doi.org/10.1016/j.prostr.2018.12.194

Cuthbertson, D., Berardi, U., Briens, C., & Berruti, F. (2019). Biochar from residual biomass as a concrete filler for improved thermal and acoustic properties. *Biomass and Bioenergy*, 120, 77–83. https://doi.org/10.1016/j.biombioe.2018.11.007

Dhyani, V., & Bhaskar, T. (2018). A comprehensive review on the pyrolysis of lignocellulosic biomass. *Renewable Energy*, 129. https://doi.org/10.1016/j.renene.2017.04.035

Falliano, D., De Domenico, D., Sciarrone, A., Ricciardi, G., Restuccia, L., Ferro, G., Tulliani, J. M., & Gugliandolo, E. (2020). Influence of biochar additions on the fracture behavior of foamed concrete. *Frattura Ed Integrita Strutturale*, 14(51), 189–198. https://doi.org/10.3221/IGF-ESIS.51.15

Glaser, B., Balashov, E., Haumaier, L., Guggenberger, G., & Zech, W. (2000). Black carbon in density fractions of anthropogenic soils of .pdf. *Organic Geochemistry*, 31, 669–678.

Glaser, B., Lehmann, J., & Zech, W. (2002). Ameliorating physical and chemical properties of highly weathered soils in the tropics with charcoal - A review. *Biology and Fertility of Soils*, 35(4), 219–230. https://doi.org/10.1007/s00374-002-0466-4

Gupta, S., & Kua, H. W. (2017). Factors Determining the Potential of Biochar As a Carbon Capturing and Sequestering Construction Material: Critical Review. *Journal of Materials in Civil Engineering*, 29(9), 04017086. https://doi.org/10.1061/(asce)mt.1943-5533.0001924

Gupta, S., Kua, H. W., & Koh, H. J. (2018a). Application of biochar from food and wood waste as green admixture for cement mortar. *Science of the Total Environment*, 619–620, 419–435. https://doi.org/10.1016/j.scitotenv.2017.11.044

Gupta, S., Kua, H. W., & Low, C. Y. (2018b). Use of biochar as carbon sequestering additive in cement mortar. *Cement and Concrete Composites*, 87, 110–129. https://doi.org/10.1016/j.cemconcomp.2017.12.009

Gupta, S., Kua, H. W., & Pang, S. D. (2018c). Healing cement mortar by immobilization of bacteria in biochar: An integrated approach of self-healing and carbon sequestration. *Cement and Concrete Composites*, 86, 238–254. https://doi.org/10.1016/j.cemconcomp.2017.11.015

Han, T. (2020). Application of peanut biochar as admixture in cement mortar. IOP Conference Series: *Earth and Environmental Science*, 531(1). https://doi.org/10.1088/1755-1315/531/1/012061

International Biochar Initiative. (2015). Standardized Product Definition and Product Testing Guidelines for Biochar That Is Used in Soil. https://biochar-international.org/wp-content/uploads/2020/06/IBI_Biochar_Standards_V2.1_Final2.pdf

International American Society for Testing and Materials. (2010). *Standard Test Method for Ash in the Analysis Sample of Coal and Coke from Coal* (ASTM D3174-04).

International American Society for Testing and Materials. (2012). *Standard Test Method for Flexural Performance of Fiber-Reinforced Concrete* (Using Beam with Third-Point Loading) (ASTM C1609M-12).

International American Society for Testing and Materials. (2014). *Standard Test Method for Compressive Strength of Hydraulic-Cement Mortars* (Using Portions of Prisms Broken in Flexure) (ASTM C349-14).

International American Society for Testing and Materials. (2015). *Standard Test Method for Flow of Hydraulic Cement Mortar* (ASTM C1437-15).

Iwuozor, K. O., Chizitere Emenike, E., Ighalo, J. O., Omoarukhe, F. O., Omuku, P. E., & George Adeniyi, A. (2022). A Review on the thermochemical conversion of sugarcane bagasse into biochar. Cleaner Materials, 6, 100162. https://doi.org/10.1016/j.clema.2022.100162

Izmir Ataturk Organized Industrial Zone. (2022, September 25). *Waste Water Treatment Plant*. http://www.iaosb.org.tr/Content/services/environment-

Izmir Water and Sewerage Administration General Directorate. (2022, September 16). *Cigli Waste Water Treatment Plant*. https://www.izsu.gov.tr/tr/TesisDetay/1/80/1

Jafri, N., Wong, W. Y., Doshi, V., Yoon, L. W., & Cheah, K. H. (2018). A review on production and characterization of biochars for application in direct carbon fuel cells. *Process Safety and Environmental Protection*, 118, 152–166. https://doi.org/10.1016/j.psep.2018.06.036

Jin, J., Li, Y., Zhang, J., Wu, S., Cao, Y., Liang, P., Zhang, J., Wong, M. H., Wang, M., Shan, S., & Christie, P. (2016). Influence of pyrolysis temperature on properties and environmental safety of heavy metals in biochars derived from municipal sewage sludge. *Journal of Hazardous Materials*, 320, 417–426. https://doi.org/10.1016/j.jhazmat.2016.08.050

Kambo, H. S., & Dutta, A. (2015). A comparative review of biochar and hydrochar in terms of production, physico-chemical properties and applications. Renewable and Sustainable *Energy Reviews*, 45, 359–378. https://doi.org/10.1016/j.rser.2015.01.050

Kan, T., Strezov, V., & Evans, T. J. (2016). Lignocellulosic biomass pyrolysis: A review of product properties and effects of pyrolysis parameters. Renewable and Sustainable *Energy Reviews*, 57, 1126–1140. https://doi.org/10.1016/j.rser.2015.12.185

Kanojia, A., & Jain, S. K. (2017). Performance of coconut shell as coarse aggregate in concrete. *Construction and Building Materials*, 140, 150–156. https://doi.org/10.1016/j.conbuildmat.2017.02.066

Kantarli, I. C., & Yanik, J. (2009). Use of waste sludge from the tannery industry. *Energy and Fuels*, 23(6), 3126–3133. https://doi.org/10.1021/ef8011068

Kawashima, S., Hou, P., Corr, D. J., & Shah, S. P. (2013). Modification of cement-based materials with nanoparticles. *Cement and Concrete Composites*, 36(1), 8–15. https://doi.org/10.1016/j.cemconcomp.2012.06.012

Khan, T. A., Saud, A. S., Jamari, S. S., Rahim, M. H. A., Park, J. W., & Kim, H. J. (2019). Hydrothermal carbonization of lignocellulosic biomass for carbon rich material preparation: A review. *Biomass and Bioenergy*, 130(October 2018), 105384. https://doi.org/10.1016/j.biombioe.2019.105384

Khushnood, R. A., Ahmad, S., Restuccia, L., Spoto, C., Jagdale, P., Tulliani, J. M., & Ferro, G. A. (2016). Carbonized nano/microparticles for enhanced mechanical properties and electromagnetic interference shielding of cementitious materials. *Frontiers of Structural and Civil Engineering*, 10(2), 209–213. https://doi.org/10.1007/s11709-016-0330-5

Kruse, A., & Dahmen, N. (2018). Hydrothermal biomass conversion: Quo vadis? *Journal of Supercritical Fluids*, 134, 114–123. https://doi.org/10.1016/j.supflu.2017.12.035

Krysanova, K., Krylova, A., Kulikova, M., Kulikov, A., & Rusakova, O. (2022). Biochar characteristics produced via hydrothermal carbonization and torrefaction of peat and sawdust. *Fuel*, 328, 125220. https://doi.org/10.1016/j.fuel.2022.125220

Kumar Mehta, P. (2001). Reducing the environmental Impact of Concrete, Concrete international, 23(10), 61-66.

Lee, J., Mahendra, S., & Alvarez, P. J. J. (2010). Nanomaterials in the construction industry: A review of their applications and environmental health and safety considerations. *ACS Nano*, 4(7), 3580–3590. https://doi.org/10.1021/nn100866w

Lee, Y., Eum, P. R. B., Ryu, C., Park, Y. K., Jung, J. H., & Hyun, S. (2013). Characteristics of biochar produced from slow pyrolysis of Geodae-Uksae 1. *Bioresource Technology*, 130, 345–350. https://doi.org/10.1016/j.biortech.2012.12.012

Lehmann, J. (2009). *Terra preta nova - Where to from here*? In W.I. Woods et al. (Eds.), Amazonian Dark Earths: Wim Sombroek's Vision (pp. 473–486). Springer Netherlands. https://doi.org/10.1007/978-1-4020-9031-8_28

Lehmann, J. & Joseph, S. (2009). *Biochar for environmental management: Science and technology*. Earthscan.

https://www.css.cornell.edu/faculty/lehmann/publ/First%20proof%2013-01-09.pdf

Li, L., Rowbotham, J. S., Greenwell, H. C., & Dyer, P. W. (2013). An Introduction to Pyrolysis and Catalytic Pyrolysis: Versatile Techniques for Biomass Conversion. In S. L. Suib (Ed.). *New and Future Developments in Catalysis* (pp. 173-208). Elsevier. https://doi.org/10.1016/B978-0-444-53878-9.00009-6

Li, R., Zhang, Y., Deng, H., Zhang, Z., Wang, J. J., Shaheen, S. M., Xiao, R., Rinklebe, J., Xi, B., He, X., & Du, J. (2020). Removing tetracycline and Hg(II) with ball-milled magnetic nano biochar and its potential on polluted irrigation water reclamation. *Journal of Hazardous Materials*, 384. https://doi.org/10.1016/j.jhazmat.2019.121095

Liang, C., Gascó, G., Fu, S., Méndez, A., & Paz-Ferreiro, J. (2016). Biochar from pruning residues as a soil amendment: Effects of pyrolysis temperature and particle size. *Soil and Tillage Research*, 164, 3–10. https://doi.org/10.1016/j.still.2015.10.002

Libra, J. A., Ro, K. S., Kammann, C., Funke, A., Berge, N. D., Neubauer, Y., Titirici, M. M., Fühner, C., Bens, O., Kern, J., & Emmerich, K. H. (2011). Hydrothermal carbonization of biomass residuals: A comparative review of the chemistry, processes and applications of wet and dry pyrolysis. *Biofuels*, 2(1), 71–106. https://doi.org/10.4155/bfs.10.81

Malghani, S., Gleixner, G., & Trumbore, S. E. (2013). Chars produced by slow pyrolysis and hydrothermal carbonization vary in carbon sequestration potential and greenhouse gases emissions. *Soil Biology and Biochemistry*, 62, 137–146. https://doi.org/10.1016/j.soilbio.2013.03.013

María Diaz-Montaño, D. (2022). Valorization of Biomass as a Raw Material to Obtain Products of Industrial Interest. *IntechOpen*. https://doi.org/10.5772/intechopen.104108

Mensah, R. A., Shanmugam, V., Narayanan, S., Razavi, S. M. J., Ulfberg, A., Blanksvärd, T., Sayahi, F., Simonsson, P., Reinke, B., Försth, M., Sas, G., Sas, D., & Das, O. (2021). Biochar-added cementitious materials—a review on mechanical, thermal, and environmental properties. *Sustainability*, 13(16). https://doi.org/10.3390/su13169336

Maldonado, E.A., & Olivares, F.H. (2017). Study of Fine Mortar Powder from Different Waste Sources for Recycled Concrete Production. In P. Mercader-Moyano (Ed.), *Sustainable Development and Renovation in Architecture, Urbanism and Engineering* (pp. 253-262). Springer International Publishing. https://doi.org/10.1007/978-3-319-51442-0

Mohajerani, A., Burnett, L., Smith, J. V., Kurmus, H., Milas, J., Arulrajah, A., Horpibulsuk, S., & Kadir, A. A. (2019). Nanoparticles in construction materials and other applications, and implications of nanoparticle use. *Materials*, 12(19), 3052. https://doi.org/10.3390/ma12193052

Mrad, R., & Chehab, G. (2019). Mechanical and microstructure properties of biochar-based mortar: An internal curing agent for PCC. *Sustainability,* 11(9), 2491. https://doi.org/10.3390/su11092491

Mumme, J., Eckervogt, L., Pielert, J., Diakité, M., Rupp, F., & Kern, J. (2011). Hydrothermal carbonization of anaerobically digested maize silage. *Bioresource Technology*, 102(19), 9255–9260. https://doi.org/10.1016/j.biortech.2011.06.099

Navaratnam, S., Wijaya, H., Rajeev, P., Mendis, P., & Nguyen, K. (2021). Residual stress-strain relationship for the biochar-based mortar after exposure to elevated

temperature. *Case Studies in Construction Materials*, 14. https://doi.org/10.1016/j.cscm.2021.e00540

Norhasri, M. S. M., Hamidah, M. S., & Fadzil, A. M. (2017). Applications of using nano material in concrete: A review. *Construction and Building Materials*, 133, 91-97. https://doi.org/10.1016/j.conbuildmat.2016.12.005

Ok, Y. Sik., Uchimiya, S. M., Chang, S. X., & Bolan, N. (2015). *Biochar : Production, Characterization, and Applications*. CRC Press Taylor & Francis Group.

Pang, S. (2019). Advances in thermochemical conversion of woody biomass to energy, fuels and chemicals. *Biotechnology Advances*, 37(4), 589–597. https://doi.org/10.1016/j.biotechadv.2018.11.004

Peterson, S. C., Jackson, M. A., Kim, S., & Palmquist, D. E. (2012). Increasing biochar surface area: Optimization of ball milling parameters. *Powder Technology*, 228, 115–120. https://doi.org/10.1016/j.powtec.2012.05.005

Praneeth, S., Saavedra, L., Zeng, M., Dubey, B. K., & Sarmah, A. K. (2021). Biochar admixtured lightweight, porous and tougher cement mortars: Mechanical, durability and micro computed tomography analysis. *Science of the Total Environment*, 750. https://doi.org/10.1016/j.scitotenv.2020.142327

Pratap, T., Patel, M., Pittman, C. U., Nguyen, T. A., & Mohan, D. (2021). Nanobiochar: A sustainable solution for agricultural and environmental applications. In A. Amrane, D. Mohan, T. A. Nguyen, A. A. Asadi, & G. Yasin (Eds.), *Nanomaterials for Soil Remediation* (pp. 501-519). Elsevier. https://doi.org/10.1016/B978-0-12-822891-3.00028-1

Qin, Y., Pang, X., Tan, K., & Bao, T. (2021). Evaluation of pervious concrete performance with pulverized biochar as cement replacement. *Cement and Concrete Composites*, 119, 104022. https://doi.org/10.1016/j.cemconcomp.2021.104022

Ramakrishna, G., & Sundararajan, T. (2019). A novel approach to rheological and impact strength of fibre-reinforced cement/cementitious composites for durability evaluation. In M. Jawaid, M. Thariq, & N. Saba (Eds.), *Durability and Life Prediction in Biocomposites, Fibre-Reinforced Composites and Hybrid Composites* (389–406). Woodhead Publishing. https://doi.org/10.1016/B978-0-08-102290-0.00017-9

Ramanayaka, S., Vithanage, M., Alessi, D. S., Liu, W. J., Jayasundera, A. C. A., & Ok, Y. S. (2020). Nanobiochar: Production, properties, and multifunctional applications. Environmental Science: *Nano*, 7(11), 3279–3302. https://doi.org/10.1039/d0en00486c

Reid, W. V., Ali, M. K., & Field, C. B. (2020). The future of bioenergy. Global Change *Biology*, 26(1), 274–286. https://doi.org/10.1111/gcb.14883

Restuccia, L., & Ferro, G. A. (2016). Promising low cost carbon-based materials to improve strength and toughness in cement composites. *Construction and Building Materials*, 126, 1034–1043. https://doi.org/10.1016/j.conbuildmat.2016.09.101

Restuccia, L., & Ferro, G. A. (2018). Influence of filler size on the mechanical properties of cement-based composites. *Fatigue and Fracture of Engineering Materials and Structures*, 41(4), 797–805. https://doi.org/10.1111/ffe.12694

Roberts, K. G., Gloy, B. A., Joseph, S., Scott, N. R., & Lehmann, J. (2010). Life cycle assessment of biochar systems: Estimating the energetic, economic, and climate change potential. *Environmental Science and Technology*, 44(2), 827–833. https://doi.org/10.1021/es902266r

Roy, P., & Dias, G. (2017). Prospects for pyrolysis technologies in the bioenergy sector: A review. *Renewable and Sustainable Energy Reviews*, 77, 59–69. https://doi.org/10.1016/j.rser.2017.03.136

Roychand, R., Patel, S., Halder, P., Kundu, S., Hampton, J., Bergmann, D., Surapaneni, A., Shah, K., & Pramanik, B. K. (2021). Recycling biosolids as cement composites in raw, pyrolyzed and ashed forms: A waste utilisation approach to support circular economy. *Journal of Building Engineering*, 38, 102199. https://doi.org/10.1016/j.jobe.2021.102199

Seow, Y. X., Tan, Y. H., Mubarak, N. M., Kansedo, J., Khalid, M., Ibrahim, M. L., & Ghasemi, M. (2022). A review on biochar production from different biomass wastes by recent carbonization technologies and its sustainable applications. *Journal of Environmental Chemical Engineering*, 10(1), 107017. https://doi.org/10.1016/j.jece.2021.107017

Shafigh, P., Jumaat, M. Z., Mahmud, H. Bin, & Alengaram, U. J. (2013). Oil palm shell lightweight concrete containing high volume ground granulated blast furnace slag. *Construction and Building Materials*, 40, 231–238. https://doi.org/10.1016/j.conbuildmat.2012.10.007

Shah, U. V., Wang, Z., Olusanmi, D., Narang, A. S., Hussain, M. A., Tobyn, M. J., & Heng, J. Y. Y. (2015). Effect of milling temperatures on surface area, surface energy and cohesion of pharmaceutical powders. *International Journal of Pharmaceutics*, 495(1), 234-240. https://doi.org/10.1016/j.ijpharm.2015.08.061

Shilar, F. A., Ganachari, S. V., & Patil, V. B. (2022). Advancement of nano-based construction materials-A review. *Construction and Building Materials*, 359, 129535. https://doi.org/10.1016/j.conbuildmat.2022.129535

Sirico, A., Bernardi, P., Belletti, B., Malcevschi, A., Dalcanale, E., Domenichelli, I., Fornoni, P., & Moretti, E. (2020a). Mechanical characterization of cement-based materials containing biochar from gasification. *Construction and Building Materials*, 246, 118490. https://doi.org/10.1016/j.conbuildmat.2020.118490

Sirico, A., Bernardi, P., Belletti, B., Malcevschi, A., Restuccia, L., Ferro, G. A., & Suarez-Riera, D. (2020b). Biochar-based cement pastes and mortars with enhanced mechanical properties. *Frattura Ed Integrita Strutturale*, 14(54), 297–316. https://doi.org/10.3221/IGF-ESIS.54.21

Smith, N. J. H. (1980). Anthrosols and Human Carrying Capacity in Amazonia. *Annals of the Association of American Geographers*, 70(4), 553–566.

Spokas, K. A. (2010). Review of the stability of biochar in soils: Predictability of O:C molar ratios. *Carbon Management*, 1(2), 289–303. https://doi.org/10.4155/cmt.10.32

Suliman, W., Harsh, J. B., Abu-Lail, N. I., Fortuna, A. M., Dallmeyer, I., & Garcia-Perez, M. (2016). Influence of feedstock source and pyrolysis temperature on biochar bulk and surface properties. *Biomass and Bioenergy*, 84, 37–48. https://doi.org/10.1016/j.biombioe.2015.11.010

Sun, J., He, F., Pan, Y., & Zhang, Z. (2017). Effects of pyrolysis temperature and residence time on physicochemical properties of different biochar types. *Acta Agriculturae Scandinavica Section B: Soil and Plant Science*, 67(1), 12–22. https://doi.org/10.1080/09064710.2016.1214745

Tomczyk, A., Sokołowska, Z., & Boguta, P. (2020). Biochar physicochemical properties: pyrolysis temperature and feedstock kind effects. *Reviews in Environmental Science and Biotechnology*, 19(1), 191–215. https://doi.org/10.1007/s11157-020-09523-3

Tripathi, M., Sahu, J. N., & Ganesan, P. (2016). Effect of process parameters on production of biochar from biomass waste through pyrolysis: A review. *Renewable and Sustainable Energy Reviews*, 55, 467–481. https://doi.org/10.1016/j.rser.2015.10.122

Turkish Grain Board. (2022, July 5). *Year 2020 Dried Apricot Industry Report*. https://tmo.gov.tr/Upload/Document/sektorraporlari/kurukayisi2020.pdf

Turkish Standards Institution. (2016). *Design of Concrete Mixtures* (TS 802).

Tursi, A. (2019). A review on biomass: Importance, chemistry, classification, and conversion. *Biofuel Research Journal*, 6(2), 962–979. https://doi.org/10.18331/BRJ2019.6.2.3

Vithanage, M., Herath, I., Joseph, S., Bundschuh, J., Bolan, N., Ok, Y. S., Kirkham, M. B., & Rinklebe, J. (2017). Interaction of arsenic with biochar in soil and water: A critical review. *Carbon*, 113, 219–230. https://doi.org/10.1016/j.carbon.2016.11.032

Wang, D., Jiang, P., Zhang, H., & Yuan, W. (2020). Biochar production and applications in agro and forestry systems: A review. *Science of the Total Environment*, 723, 137775. https://doi.org/10.1016/j.scitotenv.2020.137775

Wang, J., & Wang, S. (2019). Preparation, modification and environmental application of biochar: A review. *Journal of Cleaner Production*, 227, 1002–1022. https://doi.org/10.1016/j.jclepro.2019.04.282

Wang, L., Chang, Y., & Li, A. (2019). Hydrothermal carbonization for energy-efficient processing of sewage sludge: A review. *Renewable and Sustainable Energy Reviews*, 108, 423–440. https://doi.org/10.1016/j.rser.2019.04.011

Wang, L., Zhang, H., & Gao, Y. (2018). Effect of TiO_2 nanoparticles on physical and mechanical properties of cement at low temperatures. *Advances in Materials Science and Engineering*, 2018. https://doi.org/10.1155/2018/8934689

Weber, K., & Quicker, P. (2018a). Properties of biochar. *Fuel*, 217(1), 240–261. https://doi.org/10.1016/j.fuel.2017.12.054

Wilk, M., & Magdziarz, A. (2017). Hydrothermal carbonization, torrefaction and slow pyrolysis of Miscanthus giganteus. *Energy*, 140, 1292–1304. https://doi.org/10.1016/j.energy.2017.03.031

Woolf, D., Amonette, J. E., Street-Perrott, F. A., Lehmann, J., & Joseph, S. (2010). Sustainable biochar to mitigate global climate change. *Nature Communications*, 1(5). https://doi.org/10.1038/ncomms1053

Wu, F., Liu, C., Zhang, L., Lu, Y., & Ma, Y. (2018). Comparative study of carbonized peach shell and carbonized apricot shell to improve the performance of lightweight concrete. *Construction and Building Materials*, 188, 758–771. https://doi.org/10.1016/j.conbuildmat.2018.08.094

Xie, Y., Wang, L., Li, H., Westholm, L. J., Carvalho, L., Thorin, E., Yu, Z., Yu, X., & Skreiberg, Ø. (2022). A critical review on production, modification and utilization of biochar. *Journal of Analytical and Applied Pyrolysis*, 161, 105405. https://doi.org/10.1016/j.jaap.2021.105405

Yaashikaa, P. R., Kumar, P. S., Varjani, S., & Saravanan, A. (2020). A critical review on the biochar production techniques, characterization, stability and applications for circular bioeconomy. *Biotechnology Reports*, 28, e00570. https://doi.org/10.1016/j.btre.2020.e00570

You, S., Ok, Y. S., Tsang, D. C. W., Kwon, E. E., & Wang, C. H. (2018). Towards practical application of gasification: a critical review from syngas and biochar perspectives. *Critical Reviews in Environmental Science and Technology*, 48(22–24), 1165–1213. https://doi.org/10.1080/10643389.2018.1518860

Zhang, Z., Zhu, Z., Shen, B., & Liu, L. (2019). Insights into biochar and hydrochar production and applications: A review. *Energy*, 171, 581–598. https://doi.org/10.1016/j.energy.2019.01.035

Zhao, B., O'Connor, D., Zhang, J., Peng, T., Shen, Z., Tsang, D. C. W., & Hou, D. (2018). Effect of pyrolysis temperature, heating rate, and residence time on rapeseed stem derived biochar. *Journal of Cleaner Production*, 174, 977-987. https://doi.org/10.1016/j.jclepro.2017.11.013